DOI: 10.1002/anie.200702506

Organic Photovoltaics

Polymer–Fullerene Composite Solar Cells

*Barry C. Thompson and Jean M. J. Fréchet**

Keywords:
electron transfer · energy conversion · fullerenes · polymers · solar cells

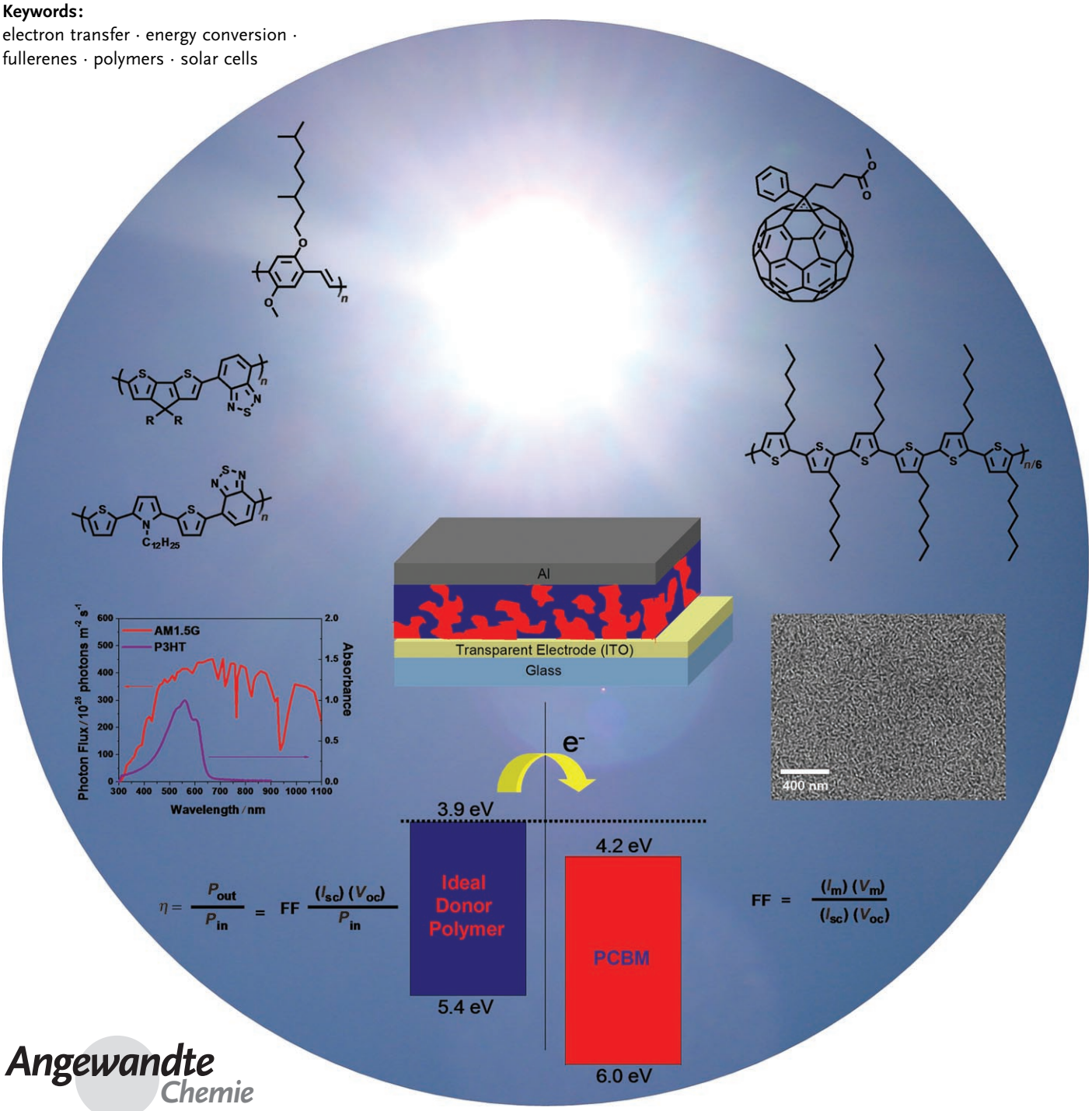

Fossil fuel alternatives, such as solar energy, are moving to the forefront in a variety of research fields. Polymer-based organic photovoltaic systems hold the promise for a cost-effective, lightweight solar energy conversion platform, which could benefit from simple solution processing of the active layer. The function of such excitonic solar cells is based on photoinduced electron transfer from a donor to an acceptor. Fullerenes have become the ubiquitous acceptors because of their high electron affinity and ability to transport charge effectively. The most effective solar cells have been made from bicontinuous polymer–fullerene composites, or so-called bulk heterojunctions. The best solar cells currently achieve an efficiency of about 5 %, thus significant advances in the fundamental understanding of the complex interplay between the active layer morphology and electronic properties are required if this technology is to find viable application.

From the Contents

1. Introduction

Organic solar cells belong to the class of photovoltaic cells known as excitonic solar cells, which are characterized by strongly bound electron–hole pairs (excitons) that are formed after excitation with light.[1] Strongly bound excitons exist in these materials as a consequence of the low dielectric constants in the organic components, which are insufficient to affect direct electron–hole dissociation, as is found in their high dielectric inorganic counterparts. In excitonic solar cells, exciton dissociation occurs almost exclusively at the interface between two materials of differing electron affinities (and/or ionization potentials): the electron donor (or simply donor) and the electron acceptor (or simply acceptor). To generate an effective photocurrent in these organic solar cells, an appropriate donor–acceptor pair and device architecture must be selected.

In the more than 20 years since the seminal work of Tang,[2] organic solar cells have undergone a gradual evolution that has led to energy conversion efficiencies (η, see Figure 1) of about 5 %.[3–8] Two main approaches have been explored in the effort to develop viable devices: the donor–acceptor bilayer,[8–10] commonly achieved by vacuum deposition of molecular components,[11] and the so-called bulk heterojunction (BHJ),[12,13] which is represented in the ideal case as a bicontinuous composite of donor and acceptor phases, thereby maximizing the all-important interfacial area between the donors and acceptors. Polymer-based photovoltaic systems which can be processed in solution, and which generally take the form of BHJ devices, most closely conform to the ultimate vision of organic solar cells as low-cost, lightweight, and flexible devices. The real advantage of these BHJ devices, which can be processed in solution, over vacuum deposition is the ability to process the composite active layer from solution in a single step, by using a variety of techniques that range from inkjet printing to spin coating and roller casting. However, regardless of the method of preparation, one feature that extends across all classes of organic solar cells is the almost ubiquitous use of fullerenes as the electron-accepting component. The high electron affinity and superior ability to transport charge make fullerenes the best acceptor component currently available for these devices.

The state-of-the-art in the field of organic photovoltaics is currently represented by BHJ solar cells based on poly(3-hexylthiophene) (P3HT) and the fullerene derivative [6,6]-phenyl-C61-butyric acid methyl ester (PCBM), with reproducible efficiencies approaching 5 %.[3,4] To attain efficiencies approaching 10 % in such organic solar cells, much effort is required to understand the fundamental electronic interactions between the polymeric donors and the fullerene acceptors as well as the complex interplay of device architecture, morphology, processing, and the fundamental electronic processes. In this Review, recent advances directed towards the optimization of organic polymer–fullerene BHJ solar cells are critically discussed in the context of how they have redefined the fundamental understanding of energy conversion to improve performance.

2. Optimization of Organic Solar Cells on the Basis of Mechanistic Principles

Efforts to optimize the performance of organic solar cells should find their basis in the fundamental mechanism of operation. Scheme 1 illustrates the mechanism by which light energy is converted into electrical energy in the devices. The energy conversion process has four fundamental steps in the commonly accepted mechanism:[14] 1) Absorption of light and

[*] Dr. B. C. Thompson, Prof. J. M. J. Fréchet
Department of Chemistry
University of California, Berkeley
and
Division of Materials Sciences
E.O. Lawrence Berkeley National Laboratory
Berkeley, CA 94720-1460 (USA)
Fax: (+1) 510-643-3079
E-mail: frechet@berkeley.edu
Homepage: http://socrates.berkeley.edu/~jfrechet/

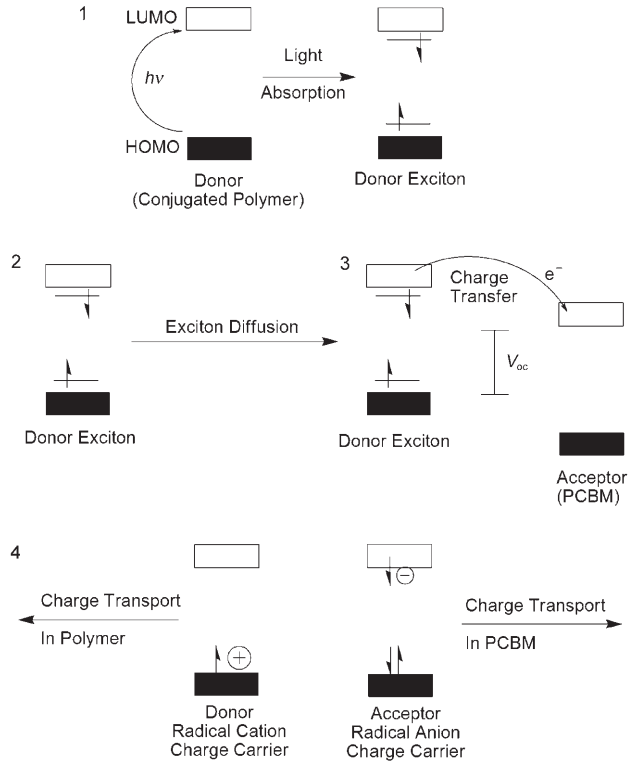

Scheme 1. General mechanism for photoenergy conversion in excitonic solar cells.

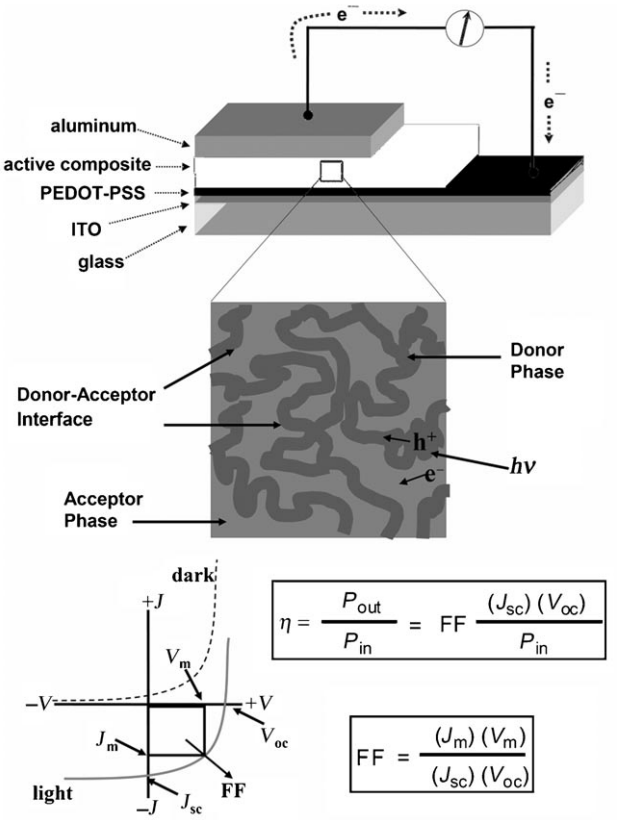

Figure 1. Schematic illustration of a polymer–fullerene BHJ solar cell, with a magnified area showing the bicontinuous morphology of the active layer. ITO is indium tin oxide and PEDOT-PSS is poly(3,4-ethylenedioxythiophene)-polystyrene sulfonate. The typical current–voltage characteristics for dark and light current in a solar cell illustrate the important parameters for such devices: J_{sc} is the short-circuit current density, V_{oc} is the open circuit voltage, J_m and V_m are the current and voltage at the maximum power point, and FF is the fill factor. The efficiency (η) is defined, both simplistically as the ratio of power out (P_{out}) to power in (P_{in}), as well as in terms of the relevant parameters derived from the current–voltage relationship.

generation of excitons, 2) diffusion of the excitons, 3) dissociation of the excitons with generation of charge, and 4) charge transport and charge collection. Figure 1 shows a schematic representation of a typical BHJ solar cell, illustrating the components involved in the mechanistic steps as well as a current–voltage curve defining the primary quantities used to validate the performance of a solar cell.

The elementary steps involved in the pathway from photoexcitation to the generation of free charges are shown in Scheme 2.[15,16] The processes can also occur in an analogous fashion in the case of an excited acceptor, and the details of these mechanistic steps have been described extensively in the literature.[16] The key point is that electron transfer is not as simple as depicted in Scheme 1. The process must be energetically favorable to form the geminate pair in step 3 of Scheme 2 and an energetic driving force must exist to separate this Coulombically bound electron–hole pair.

It is apparent that the active layer donor–acceptor composite governs all aspects of the mechanism, with the exception of charge collection, which is based on the electronic interface between the active layer composite and the respective electrode. Detailed descriptions of the steps used for device fabrication are found elsewhere.[17] Besides the fundamental mechanistic steps, the open circuit voltage

Barry C. Thompson was born in Milwaukee, Wisconsin in 1977. He studied Chemistry and Physics at the University of Rio Grande in Rio Grande, Ohio (BSc 2000) and completed his PhD in 2005 with Prof. John R. Reynolds at the University of Florida, where he studied the synthesis and electronic characterization of electroactive polymers. He is currently a post-doctoral fellow studying organic solar cells with Prof. Jean M. J. Fréchet at the University of California, Berkeley.

Jean M. J. Fréchet is the Rapoport Chair of Organic Chemistry at the University of California, Berkeley and is a director of the Molecular Foundry at Lawrence Berkeley National Laboratory. His research at the interface of organic and polymer chemistry is directed towards functional macromolecules, their design, synthesis, and applications.

$$D + A \xrightleftharpoons{h\nu} D^* + A \quad (1)$$

$$D^* + A \rightleftharpoons [D^*, A] \quad (2)$$

$$[D^*, A] \rightleftharpoons [D^{+\bullet}, A^{-\bullet}] \quad (3)$$

$$[D^{+\bullet}, A^{-\bullet}] \rightleftharpoons D^{+\bullet} + A^{-\bullet} \quad (4)$$

Scheme 2. Elementary steps in the process of photoinduced charge separation for a donor (D) and an acceptor (A): 1) Photoexcitation of the donor; 2) diffusion of the exciton and formation of an encounter pair; 3) electron transfer within the encounter pair to form a geminate pair; 4) charge separation.

(V_{oc}) is also governed by the energetic relationship between the donor and the acceptor (Scheme 1) rather than the work functions of the cathode and anode, as would be expected from a simplistic view of these diode devices. Specifically, the energy difference between the HOMO of the donor and the LUMO of the acceptor is found to most closely correlate with the V_{oc} value.[18,19]

It is therefore apparent that the choice of the components in the active layer as well as its morphology, which governs the physical interaction between the donor and acceptor, are the primary factors affecting the performance of the device. As such, the focus of this Review is the optimization and understanding of the electronic and physical interactions between polymeric donors and fullerene acceptors in BHJ solar cells. Architectural modification (such as the use of buffer layers) or the choice of electrodes are also critical aspects which will be viewed as a second level of device optimization in our discussion.

3. Electronic Donor–Acceptor Interactions

In principle, the optimization of polymer–fullerene solar cells is based on fine-tuning the electronic properties and interactions of the donor and acceptor components so as to absorb the most light, generate the greatest number of free charges, with minimal concomitant loss of energy, and transport the charges to the respective electrodes at a maximum rate and with a minimum of recombination. Such an approach, which focuses solely on the electronic characteristics of the individual components (absorption coefficient, charge carrier mobility, etc.) ignores morphological issues, which are also of critical importance in these devices and will be discussed in the following section. However, it is necessary to know the ideal electronic characteristics that each component should have for the design of the next generation, high-efficiency photovoltaic systems.

The two components required in these devices for electronic optimization are a soluble fullerene (generally a C_{60} derivative) acceptor and a polymeric donor that can be processed in solution. Fullerenes are currently considered to be the ideal acceptors for organic solar cells for several reasons. First, they have an energetically deep-lying LUMO,[20] which endows the molecule with a very high electron affinity relative to the numerous potential organic donors. The triply degenerate LUMO of C_{60} also allows the molecule to be reversibly reduced with up to six electrons, thus illustrating its ability to stabilize negative charge. Importantly, a number of conjugated polymer–fullerene blends are known to exhibit ultrafast photoinduced charge transfer (ca. 45 fs), with a back transfer that is orders of magnitude slower.[21] Furthermore, C_{60} has been shown to have a very high electron mobility of up to 1 $cm^2 V^{-1} s^{-1}$ in field-effect transistors (FETs).[22]

It is these fundamental properties, coupled with the ability of soluble fullerene derivatives to pack effectively in crystalline structures conducive to charge transport,[23] that have made fullerenes the most important acceptor materials for BHJ solar cells. The electronic structure of the fullerenes can be considered to be constant regardless of the chemical functionalization used for solubilization: for most functionalized fullerenes, the first reduction potential only varies by ± 100 mV relative to C_{60}.[18,24,25] Therefore, the constraints and requirements for the electronic band structure of an ideal polymeric donor become clear. The relationship is illustrated in Figure 2, for the example of MDMO-PPV (poly[2-methoxy-5-(3,7-dimethyloctyloxy)-1,4-phenylen]-*alt*-(vinylene)) and P3HT, two of the most commonly used donor polymers.

The first constraint is that the donor must be capable of transferring charge to the fullerene upon excitation (Scheme 1). A downhill energetic driving force is necessary for this process to be favorable and the driving force must exceed the exciton binding energy. This binding energy is the Coulombic attraction of the bound electron–hole pair in the donor, and typical values are estimated to be 0.4–0.5 eV.[26] The energetic driving force effects the dissociation of the

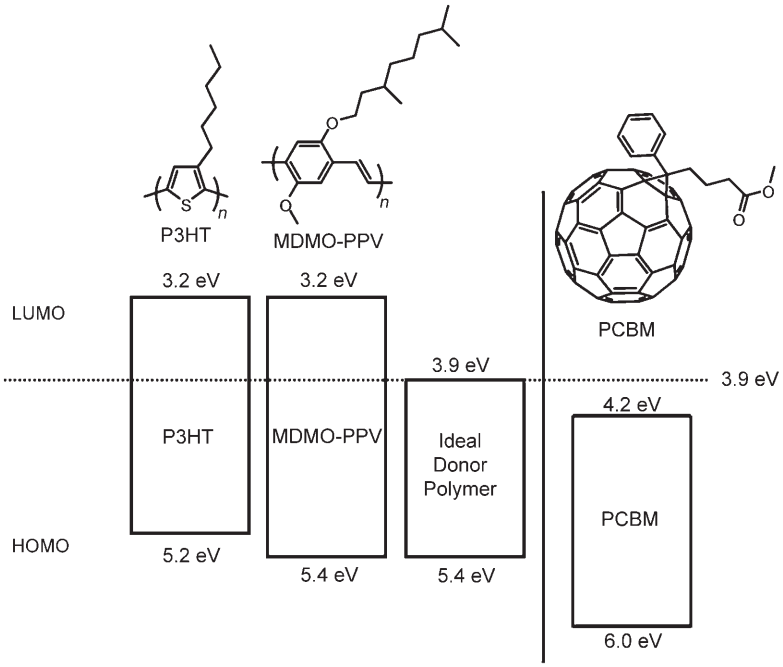

Figure 2. Band structure diagram illustrating the HOMO and LUMO energies of MDMO-PPV, P3HT, and an "ideal" donor relative to the band structure of PCBM. Energy values are reported as absolute values relative to a vacuum.

exciton with the formation of a geminate pair (step 3 in Scheme 2). An additional energetic driving force is required to separate this geminate pair bound by Coulombic forces to generate free charges. This process is aided both thermally and by the intrinsic electric field in the device.

Much more sophisticated descriptions of the energetic requirements for photoinduced electron transfer in the solid state are given elsewhere, but in general the change in the free energy on converting two neutral species into two separated charged species must be favorable (that is, exergonic).[16,27] Empirically, the overall energetic driving force for a forward electron transfer from the donor to the acceptor is represented by the energy difference (offset) between the LUMOs of the donor and acceptor. It appears that a minimum energy difference of 0.3 eV is required to affect the exciton splitting and charge dissociation.[28,29] Furthermore, an energy difference between the LUMOs that is larger than this minimum value does not seem to be advantageous, and indeed results in wasted energy that does not contribute to the device performance.[30] The ideal polymer would have a minimum energy difference between the LUMOs; in this way wasted energy upon exciton splitting would be avoided and the bandgap of the polymer would be minimized so as to maximize the absorption of light. Thus, the LUMO of an ideal polymer would reside at approximately 3.9 eV, since the LUMO energy for PCBM, the most commonly and successfully employed soluble fullerene derivative, is 4.2 eV.

The HOMO energy of the ideal donor polymer would then be determined by considering the bandgap of the polymer, and hence the absorption of light, as well as the influence on the open circuit voltage (V_{oc}). The lower the energy of the HOMO, the greater the maximum theoretically attainable V_{oc} value, but the larger the bandgap, the poorer the spectral overlap with the photon flux from the sun, which has a maximum at 1.8 eV (ca. 700 nm). A compromise is found by considering that a bandgap of about 1.5 eV is an optimal value for a polymer absorber.[31] This gives a HOMO energy of about 5.4 eV, which corresponds to a maximum attainable V_{oc} value of 1.2 V. The optimal bandgap value of 1.5 eV has been determined through a detailed analysis that balances the attainable V_{oc} value and the donor bandgap.[32] A broad absorption band for the polymer between 4.1 and 1.5 eV and a high absorption coefficient (at least 10^5 cm^{-1}) are also assumed to be a critical criteria for an ideal system. A high charge carrier mobility for the polymer commensurate with that of PCBM (10^{-3} cm^2 V^{-1} s^{-1} measured in a space–charge limited regime[33] or ca. 10^{-1} cm^2 V^{-1} s^{-1} measured in field-effect transistors[34]) is also assumed for such an ideal donor; the specifics of charge mobility will be described in the following sections.

Several studies have been aimed at designing optimal donor polymers for PCBM, either on a theoretical or empirical basis, by using the mechanism of solar cell operation presented in Scheme 1, and in an analogous manner as the above discussion.[30,32,35] Specific concerns about the electronic interaction between the polymer and the fullerene have also been raised recently on the basis of a growing understanding of the fundamental photoconversion process, which challenges the simplistic mechanism presented in Scheme 1.

The first concept that must be considered is the precise sequence of events that lead to charge separation following the absorption of light and the generation of an exciton in the donor polymer. In the generally accepted mechanism, direct electron transfer from the donor to the acceptor occurs following the diffusion of the exciton to the donor–acceptor interface. However, another possible mechanism (Scheme 3)

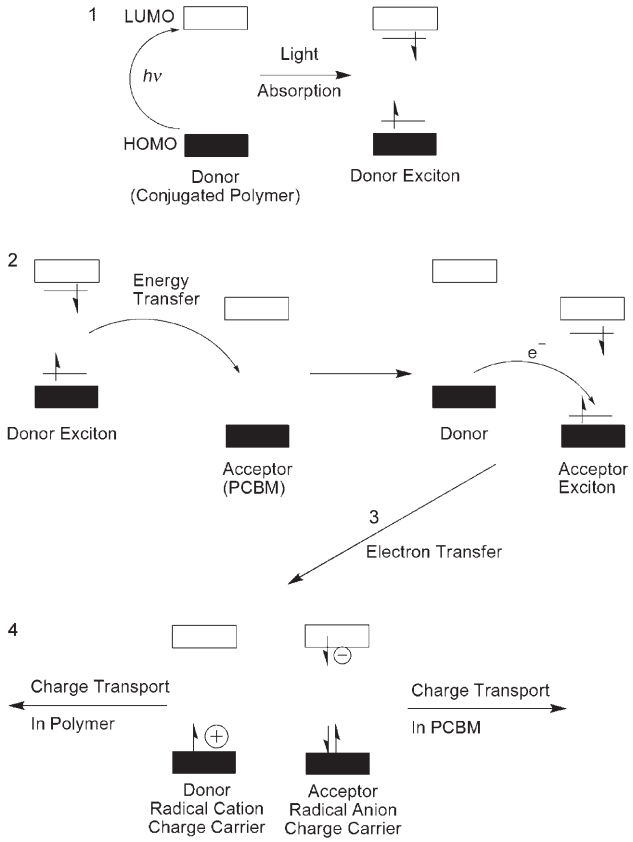

Scheme 3. FRET mechanism for the conversion of solar energy.

involves a Förster resonance energy transfer (FRET) from the donor to the acceptor after excitation, thus generating an exciton in the acceptor. Electron transfer from the donor to the acceptor by oxidation of the donor by the excited-state acceptor then leads to a free electron and free hole, if the difference between the HOMOs of the two components is sufficient to drive the charge transfer. This process has been observed to operate in covalent oligomer–fullerene dyads in solution[36] and has recently been observed for fullerenes in the solid state.[37]

In the latter case, a dye (Nile Red) was blended with PCBM in a polystyrene matrix. The small dye molecule was used to approximate the electronic absorption and emission characteristics of a typical conjugated polymer, while retaining the ability to spatially separate the small molecule donor from PCBM in a polymer matrix. The emission of the dye overlaps well with the weak absorption of PCBM in the 500–700 nm range (a requirement for resonance energy transfer). The substantial fluorescence quenching in the films was taken as clear evidence of resonance energy transfer from the Nile

Red to the PCBM. The main conclusion of such studies is that resonance energy transfer can increase the effective diffusion length of the exciton in conjugated polymers beyond the approximate limit of 5 nm.[38] Otherwise domain sizes on the order of about 10 nm would be required to avoid having the performance of the device limited by exciton diffusion. Besides increasing the effective exciton diffusion length, the exploration of donor–acceptor pairs that give effective resonance energy transfer, followed by charge transfer, may allow trapped excitons at low-energy sites to be harvested. It should be noted that polymer donors with bandgaps of less than 1.8 eV will show emission that will not overlap with the C_{60} absorption, thus precluding the operation of this mechanism.

While the ultimate outcome of either mechanism (Schemes 1 and 3) is essentially equivalent, the extent to which either mechanism is operating can have profound effects on the design of next-generation photovoltaic materials, and depend on the extent to which an RET-based mechanism could enhance the exciton diffusion length in a polymer. Furthermore, the action of such a mechanism implies that the energy difference between the HOMOs of the donor and acceptor is also a relevant parameter, rather than simply the difference between the LUMOs. The requisites for an RET-based donor–acceptor pair are a high photoluminescence quantum yield for the donor and a strong overlap between the donor emission and acceptor absorption.

There is another issue that affects the design of conjugated polymers for use with fullerene acceptors that goes beyond the simplistic HOMO–LUMO energy relationship shown in Scheme 1. A variety of energetic considerations that extend beyond the simple difference in the LUMOs deemed necessary for charge transfer must be considered for any donor–acceptor pair. In a recent study,[39] two alkylthiophene polymers with HOMO energies lying lower than P3HT were blended with PCBM to study the energy- and charge-transfer processes relative to the P3HT/PCBM system.

In polymer 1 (P1 in Scheme 4a), which had the lowest lying HOMO (5.6 eV, although it should be noted that PCBM was taken to have a LUMO of 3.7 eV), the formation of polymer triplet states in PCBM blends was determined by photoinduced absorption, while blends with P2, with a HOMO of 5.4 eV, showed PCBM triplet states. The results can be explained by considering the triplet energies of the materials involved as well as the charge-separated state (CS state) for the donor–acceptor pairs (Scheme 4). The energy of the CS state is taken as the energy difference between the donor HOMO and the acceptor LUMO, and can be represented as the geminate pair shown in Scheme 2. It should be noted that the CS state can take the form of an exciplex (an excited state bound donor–acceptor pair in which partial charge transfer beteen the components is observed) through relaxation of the geminate pair.[40] Following excitation of the donor, charge transfer to the acceptor yields a CS state, which can have several fates, depending on its energy relative to the triplet energies of the donor and acceptor involved. If the CS state is lower in energy than the two triplet states (as in the case of P3HT and PCBM) the CS state can lead to free charge carriers. However, if the CS state is higher

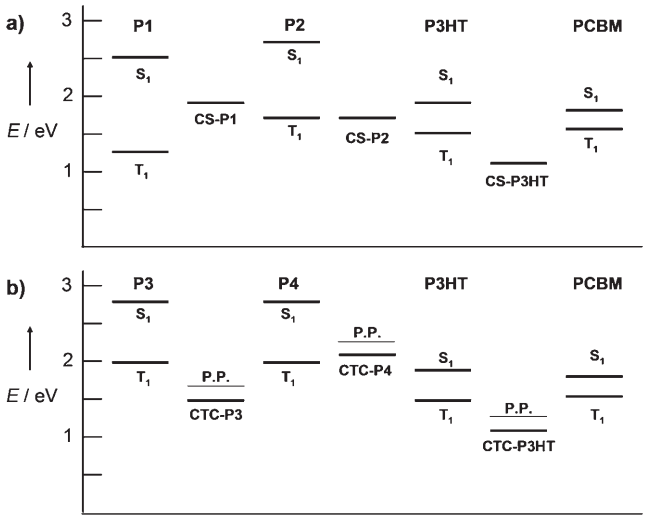

Scheme 4. a) Energy level diagram illustrating the influence of the CS state energy and the triplet energies in a polymer–fullerene pair on the likelihood of the generation of free charge carriers. Polymer 1 (P1) has a CS state energy (CS-P1) of 1.9 eV for the P1-PCBM pair as determined by E_{LUMO}(acceptor)$-E_{HOMO}$(Donor); CS-P2 is 1.7 eV and CS-P3HT is ca. 1 eV. The approximate singlet (S_1) and triplet (T_1) energies are shown for each component, with T_1 for PCBM at ca. 1.55 eV. b) An analogous energy level diagram illustrating the influence of the CTC and T_1 energies in a polymer–PCBM pair on the likelihood of the generation of free charge carriers. The CTC energies for P3, P4, and P3HT are estimated in an analogous way as the CS energies to be 1.5 eV, 2.1 eV, and ca. 1 eV. For the P3-PCBM pair, the CTC is the lowest energy state, whereas for the P4-PCBM pair, the PCBM T_1 is lowest.

in energy than the triplet states available for population (as is the case for P1 and P2, Scheme 4a), intersystem crossing within the CS state, followed by energy transfer is favored, which leads to the generation of triplet states rather than free charges. This study underscores the importance of considering all the energy levels in the specific donor–acceptor pair.

Recent evidence has also shown that awareness of other interfacial intermediate states is critical when selecting effective polymeric donors. In a recent publication,[41] evidence is given for the existence of a ground-state charge-transfer complex (CTC), generated by the interaction of the donor and the acceptor. The CTC is also defined as having energy equal to the energy difference between the donor HOMO and the acceptor LUMO. The main difference here is that the CTC state is a ground state that can absorb and emit light. The CTC is very similar to an exciplex, with the main difference that an exciplex is an excited-state species only, and is not coupled to the ground state.[42] The existence of a CTC in polymer–fullerene composites has been detected by photothermal deflection spectroscopy (PDS), used to observe the absorbance of the ground state species, and by photoluminescence, used to detect emission. In essence, the CTC is an uncharged energetic state defined by a ground-state coupling of the HOMO of the donor and the LUMO of the acceptor, but does not constitute a ground-state charge-transfer species.

Scheme 4b illustrates how the existence of a CTC is expected to influence the photoenergy conversion and also

illustrates a complex interplay of energetic events that must be considered when designing a new polymeric donor. In the example shown in Scheme 4b, the singlet (S_1) and triplet (T_1) energies for the three polymers P3, P4, and P3HT as well as of PCBM are shown relative to the CTC and polaron pair (P.P.; also referred to as a geminate pair) energies for the two distinct cases. The energy level of the polaron pair is shown to be slightly higher than the CTC simply to indicate that energy is required to generate the polaron pair from the CTC, although the actual energy of the free, relaxed polaron pair may be lower than that of the CTC.

The consequence of photoexcitation of the donor can thus fall into two categories depending on the energetic relationship of the CTC relative to the other available energy levels. The CTC of P3 (a copolymer of fluorene and triphenylamine) has an energy of 1.5 eV, which places it below all the other states (the T_1 state of PCBM is just above at ca. 1.55 eV). As a consequence, P3 shows strong photoluminescence quenching in blends with PCBM and allows the generation of photocurrent in solar cells. In the case of P4 (poly(9,9-dioctylfluorenyl-2,7-diyl), PFO), for which the CTC is at 2.1 eV, photoexcitation of a blend with PCBM leads to emission from the PCBM singlet state (ca. 1.7 eV), with no photovoltaic activity. In this case, excitation of the donor is followed by energy transfer to the PCBM, which could then fluoresce (observed) or undergo intersystem crossing (not observed). The results presented in this study for three different polymers support the existence of a CTC and its role in the charge- and energy-transfer process. Further investigation will reveal more about the nature of this CTC and the role it plays in polymer–fullerene solar cells. Note that in both Scheme 4a and b, the energetic relationship of the P3HT-CS and the P3HT-CTC to PCBM is ideal for generating geminate pairs.

It is interesting to note that both the RET mechanism from Scheme 3 and the mechanisms of Scheme 4 have common aspects that also differentiate them from the simple mechanism presented in Scheme 1. For the RET, CS, and CTC models, the HOMO energy of the donor polymer is critical not just for how it influences the V_{oc} value but also for determining whether or not photocurrent will be generated. These studies also indicate that there is a minimum HOMO energy that polymers can possess for the generation of efficient charge carriers in composites with PCBM. If the HOMO is too low in energy, the CS state (or the CTC) will be high in energy, and lie above the S_1 and/or T_1 state(s) of PCBM, thereby leading to the possibility of another mechanism for energy loss. When the LUMO energy of PCBM is taken as 4.2 eV and the T_1 state of PCBM is taken as 1.55 eV (assumed on the basis of the reported T_1 energy for C_{60}[43]), the CS state or CTC must lie at 1.5 eV or lower, thus placing the lowest donor HOMO at 5.7 eV. This situation also appears to place an upper limit on the attainable V_{oc} value in polymer–PCBM solar cells. Based on the ideal band structure for a donor polymer discussed previously, the HOMO energy of 5.4 eV would give a CS state (and CTC) with an energy of 1.2 eV, which would lie well below the T_1 state of PCBM at about 1.55 eV.

The ultimate mechanism that operates may be one of the three presented here or a combination of all three, and the mechanism that predominates may vary from polymer to polymer. Future studies will be required to answer this question, but awareness of all the possible factors that are important will help in the design of better donors for PCBM, and indeed other acceptors.

4. Morphology

Even if the donor and acceptor have an ideal electronic relationship, the performance of BHJ solar cells still depends on the physical interaction of the donor and acceptor components, which is manifested by the composite morphology. The ideal bulk-heterojunction solar cell is defined as a bicontinuous composite of donor and acceptor with a maximum interfacial area for exciton dissociation and a mean domain size commensurate with the exciton diffusion length (5–10 nm). The two components should phase-segregate on a suitable length scale to allow maximum ordering within each phase and thus effective charge transport in continuous pathways to the electrodes so as to minimize the recombination of free charges. The composite should also be formed from solution and self-assemble into the most favorable morphology with the minimal application of external treatments, as well as having long-term stability. Such requirements necessitate that the proper balance between the mixing and demixing of the two components can be achieved.

The morphology of the active layer depends on the interplay between a number of intrinsic and extrinsic variables. The intrinsic properties are those that are inherent to the polymer and the fullerene, as well as the fundamental interaction parameters between the two components. These include the crystallinity of the two materials as well as their relative miscibility. The extrinsic factors include all the external influences associated with device fabrication, such as solvent choice, overall concentration of the blend components, deposition technique (spin coating, ink-jet printing, roller casting, etc.), solvent evaporation rate, as well as thermal and/or solvent annealing. It is clear that the number of factors affecting the morphology of the active layer is immense and specific to the polymer–fullerene pair used. These factors are best discussed in the context of the two specific components, and the two current prototypical examples of BHJ solar cells MDMO-PPV/PCBM and P3HT/PCBM will be discussed below.

From a morphology standpoint, one of the most thoroughly studied donor–acceptor pairs for BHJ solar cells is the MDMO-PPV/PCBM couple, and has recently been reviewed.[44,45] A detailed treatment will not be given here, but several key points about BHJ morphology and polymer–fullerene interactions in general are illustrated effectively by this system.

The first important point is the effect of the solvent on the morphology of the active layer and the performance of the device. It was observed that casting the active layer blend from toluene gave power conversion efficiencies of about 0.9% with a 1:4 weight ratio of polymer to fullerene. When the solvent was changed to chlorobenzene, the efficiency

dramatically improved to 2.5%.[46] Spectroscopic studies proved that the difference was purely morphological. In the toluene-cast films it was observed that micrometer-sized PCBM clusters are embedded in a polymer "skin".[47] This arrangement gives rise to a non-bicontinuous blend, in which fullerene photoluminescence is not fully quenched by the polymer, thus indicating the macroscale phase segregation in the system. In the chlorobenzene-cast films, PCBM clusters with sizes less than 100 nm are observed in a significantly more homogenous and bicontinuous composite.

The vastly improved performance of the films cast from chlorobenzene can be attributed to two factors: 1) the length scale of phase segregation is the same order of magnitude as the exciton diffusion length, and 2) the more bicontinuous nature of the films facilitate charge transport. The cause for the vast differences in morphology can be attributed primarily to the greater solubility of PCBM in chlorobenzene than in toluene (4.2 wt% in chlorobenzene but only about 1 wt% in toluene).[44] The consequence of this is that the toluene solution contains preformed clusters which lead to the large cluster size observed in the toluene-cast films.

The above example clearly indicates the importance of solvent choice for generating homogenous solutions. Another decisive factor in determining the film morphology is the inherent miscibility of the two components. This has the consequence that the morphology depends on the composition and that there is an optimum composition for maximum device performance. The inherent miscibility is a thermodynamic aspect of the interaction of the polymer and the fullerene which is also dependent on the solvent choice. It is apparent in the MDMO-PPV/PCBM system that the two components tend toward phase segregation at the compositions that are relevant for device fabrication because of an inherent immiscibility of the components. This is evidenced by the high weight percentage of fullerene required relative to the polymer to generate a percolated network. This lack of miscibility is exacerbated by thermal annealing, which leads to macrophase separation even at short annealing times below the glass temperature (T_g) of the polymer.[48] These results illustrate the fact that a polymer–fullerene blend with nanoscale phase-separated domains is thermodynamically unstable and can only be generated by kinetic trapping of the preferred morphology (through control of the rate of solvent evaporation from a solvent in which both components are highly soluble).

To enable comparison with other polymer–fullerene BHJ solar cells, the parameters for the MDMO-PPV/PCBM solar cells are summarized. Films spin-cast form chlorobenzene are characterized by the parameters $V_{oc} = 0.82$ V, $J_{sc} = 5.25$ mA cm^{-2}, and FF = 0.61, which lead to a device efficiency of 2.5%[46] under AM1.5 conditions at 80 mW cm^{-2} (with a spectral mismatch factor of 0.753 applied). To be technically correct, AM1.5 measurements should be performed at 100 mW cm^{-2} and should be corrected for any spectral mismatch induced from the light source or calibration of the light source. The technical procedure for collecting highly accurate data has already been published.[49,50] In this Review, all the efficiencies reported are obtained under AM1.5 conditions with intensities of 80–100 mW cm^{-2}, irrespective of whether a spectral mismatch factor was applied or not.

The most effective polymer–fullerene combination for BHJ solar cells is the P3HT/PCBM system, with efficiencies of 4–5%.[3–5,51–53] A general reproducibility of values greater than 5% has not yet been achieved, but values approaching 5% are becoming more commonplace with P3HT/PCBM solar cells. While the electronic interaction between these two components is certainly favorable, as discussed in the previous section, it is ultimately the morphology of the active layer (and the ability to control this morphology) that has led to the best performance in this type of solar cell.

Several levels of optimization have been employed in the most efficient versions of the P3HT/PCBM BHJ solar cells. The first is the weight ratio of the two materials. In contrast to the MDMO-PPV/PCBM system where a 1:4 blend of polymer to fullerene was employed because of miscibility issues, a 1:1 ratio[4] or 1:0.8 ratio[3,5] of polymer to fullerene was found to be optimal. However, several reports indicate that ratios as low as 1.0:0.6 or 1.0:0.43 also lead to optimized performance.[51,54] These results point to a much greater inherent miscibility between P3HT and PCBM than is observed for MDMO-PPV and PCBM. Chlorobenzene is generally used as the solvent[3,5] because both PCBM and P3HT are soluble, although 1,2-dichlorobenzene has been reported to give devices with comparable performance.[4,57]

The best devices[3] are obtained from a solution of 10 mg mL^{-1} P3HT and 8 mg mL^{-1} PCBM in chlorobenzene, and after spin coating a relatively homogenous composite film is formed in which little or no phase segregation is observed beyond the length scale of a few nanometers. Such untreated films were observed by Ma et al. to give energy conversion efficiencies of less than 1% under AM1.5 conditions,[3] although it should be noted that several research groups have measured efficiencies of greater than 2%. The difference in the efficiencies can be explained by differences in the techniques used to prepare the films, as will be discussed below. The poor performance of as-cast films is generally attributed to a poorly developed morphology that consists of an intimately mixed composite of donor and acceptor rather than a bicontinuous network with well-developed and ordered pathways for the transport of charge. The intimate mixing in the as-cast films has been further confirmed on the molecular level by using 2D NMR techniques, which indicate a high degree of interaction between the hexyl side chains of the polymer and the fullerene cages.[55]

This intimate and homogenous mixing of components in spin-coated films confirms that the interaction between P3HT and PCBM is more favorable than that between MDMO-PPV and PCBM. It also suggests that the kinetically trapped morphology initially obtained is unstable to phase segregation, being driven by the strong tendency of the two components to crystallize independently. The judicious application of an external variable, such as heat or solvent vapour, can drive the phase segregation of P3HT and PCBM into bicontinuous domains.

A variety of methods have been used to optimize the morphology of these films to obtain the best solar cell performance. The most commonly used technique involves

thermal annealing, as first reported by Padinger et al.[56] Heating the active layer of the device to a temperature greater than the glass temperature T_g of P3HT (the T_g value of P3HT has been reported to be 110 °C,[57] but no clear feature is observed and thus the precise value is still under debate) allows 1) the polymer chains to reorganize and 2) the fullerene molecules to freely diffuse into the composite and reorder in a more thermodynamically favorable way. Figure 3

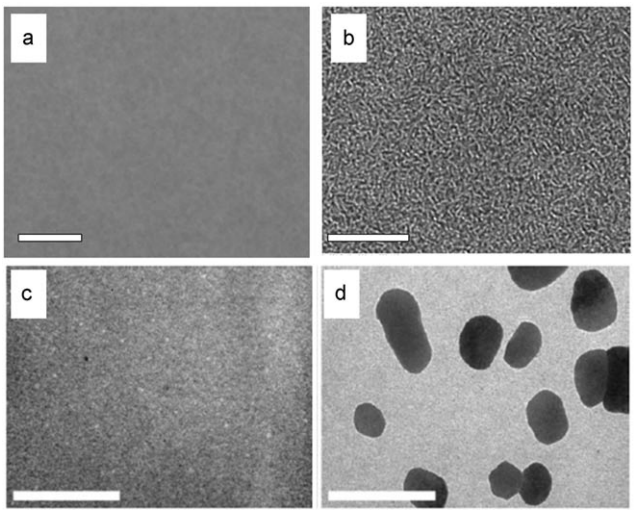

Figure 3. TEM images of a P3HT/PCBM composites. a) 1:1 blend of Rieke P3HT (regioregularity = 92%) and PCBM prior to annealing (scale bar 0.5 μm); b) the same sample after annealing at 150 °C for 30 minutes (scale bar 0.5 μm). (Reproduced with permission from *J. Am. Chem. Soc.* **2006**, *128*, 13988–13989.) c) 1:1 blend of P3HT (regioregularity > 96%) and PCBM prior to annealing (scale bar 2 μm); d) the same sample after annealing at 140 °C for 1 h (scale bar 2 μm). (Reproduced with permission from *Adv. Mater.* **2006**, *18*, 206–210.)

illustrates this change in morphology as monitored by transmission electron microscopy (TEM). Figure 3a and b shows that thermal annealing of a 1:1 blend of P3HT (Rieke Metals) and PCBM leads to the development of a nanoscale phase-separated bincontinuous network. Figure 3c and d show the case in which thermal annealing has induced phase separation and the generation of macroscopic domains of a 1:1 blend of P3HT and PCBM. The relationship between the P3HT structure and the composite thermal stability will be discussed later in this section.

A detailed investigation by TEM and selected-area electron diffraction (SAED)[58] of the morphological consequences of thermal annealing shows the growth of large P3HT fibrillar crystals (lamellar in nature) from the smaller fibrillar structures generated upon spin casting. The fibrils grow in the direction in the interchain π axis of the polymer. Since P3HT crystallizes faster and more readily than PCBM, the growth of crystalline P3HT domains upon thermal treatment is accompanied by free diffusion of the fullerene molecules within the composite film, thus leading to aggregation of PCBM in domains that crystallize slowly. A bicontinous network with nanometer-scale phase segregation is obtained by judicious application of this thermal annealing step, in which the heating time and temperature is temperature is carefully controlled. The ability to control the domain size at short annealing times—a feature not attainable with any level of thermal annealing in the MDMO-PPV/PCBM system—is attributed to inhibition of the fast diffusion of PCBM by the rapidly formed P3HT fibril network acting as boundaries and enforcing a measure of control over the degree of phase segregation. Once a highly ordered bicontinuous network of P3HT and PCBM has been induced by thermal annealing, device efficiencies jump to the 4–5% range that characterizes the state-of-the-art of this technique today. Figure 4 illustrates the effect of annealing on the current–voltage curve and the external quantum efficiency (EQE, also IPCE = incident photon-to-current efficiency; the ratio (in %) of electrons harvested to incident photons at a single wavelength) for typical P3HT/PCBM solar cells. The data show that annealing results in significant improvements in the conversion of harvested photons into harvested charges at all wavelengths across the composite absorption spectrum.

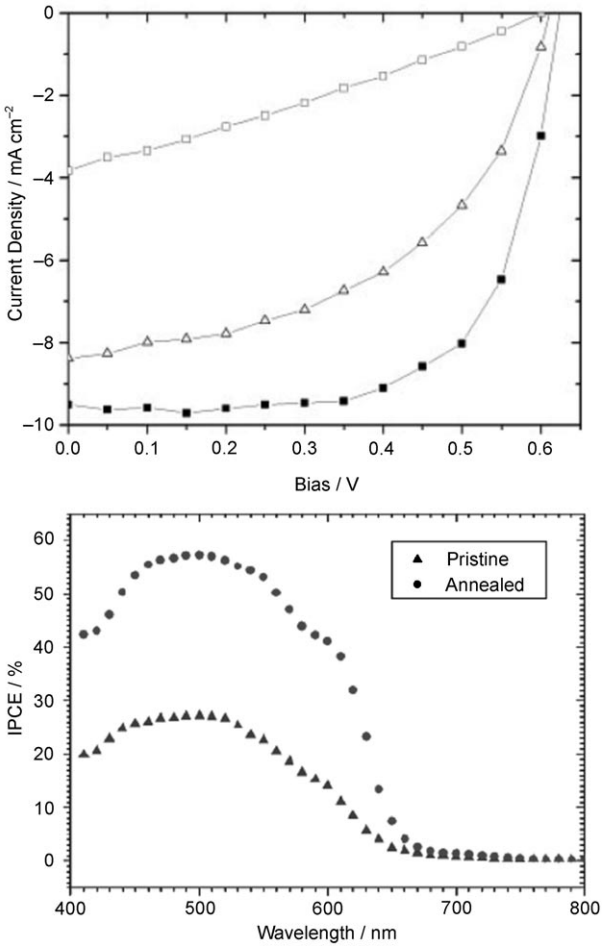

Figure 4. Top): Current–voltage curve for a P3HT/PCBM solar cell prior to annealing (□, $\eta = 0.82\%$), after annealing at 70 °C for 30 min (△, $\eta = 3.2\%$), and 150 °C for 30 minutes (■, $\eta = 5\%$). (Reproduced with permission from *Adv. Funct. Mater.* **2005**, *15*, 1617–1622.) Bottom: EQE spectrum for a P3HT/PCBM composite solar cell before (▲) and after thermal annealing (●). (Reproduced with permission from *Nano Lett.* **2005**, *5*, 579–583.)

The precise details of how the thermal annealing treatment should be applied vary from report to report, and reflect the fact that experimental parameters, such as differences in polymer sample, spin-coating conditions, polymer–fullerene ratio, have a strong effect on the initial morphology after spin coating as well the consequences of thermal annealing. In general though, annealing temperatures between 100 and 150 °C are applied for as little as 1 minute or up to 2 hours. One critical point to mention is that annealing prior to deposition of the cathode (generally aluminum) results in poorer device performance than when annealing is performed after deposition of the cathode.[59–61] A so-called confinement effect is responsible for this difference in performance and tends to reduce the length scale and degree of phase segregation.

Similar improvements in device efficiency can be observed with other techniques such as solvent annealing or the controlled evaporation of solvent from the cast films. Yang and co-workers have pioneered the use of controlled solvent evaporation during film formation in P3HT/PCBM solar cells.[4,62] It is observed that when films of a 1:1 blend of P3HT and PCBM are spin coated from a 1,2-dichlorobenzene solution the rate of solvent evaporation prior to deposition of the cathode has a strong effect on the performance of the device. When the cast film is allowed to dry in a covered petri dish over a 20-minute period prior to Al deposition, an energy conversion efficiency of 3.52 % is measured with no thermal annealing. If the same film is dried in a nitrogen flow for three minutes, the maximum energy conversion efficiency is reduced to 2.80 %, while acceleration of the rate of solvent evaporation by heating the substrate to 50 or 70 °C leads to further efficiency reductions to 2.10 and 1.36 %, respectively. This experiment suggests that both the presence and residence time of solvent molecules in the film contribute to phase reorganization, and leads to results that are roughly similar to those obtained by thermal annealing.

Further experiments showed that the best device (3.52 % efficiency) obtained by solvent evaporation benefited from subsequent thermal annealing at 110 °C for 10 minutes: its efficiency increased to 4.37 %. This finding suggests that either the evaporation time of 20 minutes was insufficient to allow optimal reorganization of the morphology, or that thermal annealing provides a more effective driving force for reorganization of the film. Longer annealing times resulted in a decrease in the peak efficiency of this device, likely as a result of phase segregation taking place on a larger than optimal length scale. Similar results have also been observed when a true solvent annealing step was employed.[63]

Other studies have suggested that the performance of devices obtained by solvent annealing can exceed that of thermally annealed devices. Thus, thermal annealing at 110 °C for 4 minutes of a 1:1 P3HT/PCBM film cast from chloroform led to efficiencies of 3.1 %, while devices cast from the same blend in dichlorobenzene and allowed to evaporate overnight in a sealed petri dish overnight with no thermal annealing had efficiencies of 3.7 %.[64] Film thickness also appears to be an important variable, as it was shown in the same study that the optimal film thickness for quickly evaporated films was about 100 nm, whereas the solvent annealed films were optimal at about 300 nm.

Such disparity appears to be directly related to differences in in the mobility of the charge carriers in the active layers. For the devices cast from chloroform and annealed at 110 °C, the hole mobility measured in the space–charge limit (SCL) was found to be $1.1 \times 10^{-4}\,cm^2 V^{-1} s^{-1}$, whereas the thicker film, in which dichlorobenzene was slowly evaporated, showed a value of $5 \times 10^{-3}\,cm^2 V^{-1} s^{-1}$. This constitutes an increase in the hole mobility by a factor of 45, and can be attributed to a more favorable reorganization of P3HT during the slow solvent evaporation process. The higher mobility allowed a thicker film to be used, which resulted in an increased photocurrent as a result of increased absorption (until the space–charge limit was reached). At the space–charge limit, holes are generated in the active layer at a rate that exceeds the rate at which they can be transported out of the film. The build-up of space charge lowers the fill factor and device efficiency.

All of these results emphasize the importance of an annealing step for reorganizing the polymer chains to achieve maximum mobility of the charge carriers. They also highlight the importance of the optimization of the film thickness, which influences the annealing conditions used. For example, Li et al.[60] reported that optimal performance (4 %) in 1:1 blends of P3HT and PCBM is achieved with 63-nm-thick films, which are thermally annealed at 110 °C for 10 minutes. The use of 155-nm-thick films under the same conditions led to efficiencies of only about 2 %. It appears that it is currently difficult to establish universal optimum values for certain parameters in device construction because of variations in polymer structure (regioregularity, molecular weight, polydispersity, etc.) and processing conditions.

While the above results do not necessarily confirm whether solvent or thermal annealing of the film is the superior method, they confirm the great importance of morphological control within the active layers to generate highly efficient devices. The primary consequences of either type of annealing are, firstly, an increase in the absorption of light as a result of an induced red-shift in the absorption onset (which broadens the polymer absorption spectrum) caused by the greater ordering in the polymer backbone and higher degree of intermolecular ordering and concomitant increase in the absorption coefficient of the ordered polymer.[65,66] Specifically, it has been observed that the annealed P3HT/PCBM blend is capable of absorbing 60 % more photons than the un-annealed blends. Secondly, there is an increase in the induced mobility of the charge carriers in the more highly ordered film, as described above.

The "molecular" optimization of both active layer components has also played a large role in the evolution of organic photovoltaic devices. While PCBM has been found to produce the best results to date in photovoltaic devices, no extensive testing of alternative fullerene structures has been reported, and it is unclear whether PCBM possesses any inherent advantage over other potential fullerenes. In fact, recent reports of devices prepared from alternatively substituted soluble fullerene derivatives in combination with P3HT have shown efficiencies of around 4.5 % under AM1.5

conditions, with little optimization.[67] This finding indicates that further tuning of the fullerene structure to match the requirements of the polymeric donor may lead to composite films with enhanced performances.

In contrast, a great deal of optimization has gone into the polymer component, which has led to the widespread use of P3HT in solar cells. The primary variables for polymers of this type are its molecular weight and regioregularity (RR, defined as the percentage of head-to-tail linkages in the polymer). Several studies have examined the effects of these variables on the intrinsic properties of P3HT both in pristine films and in BHJ solar cells with PCBM. In both types of films, the relevant parameters for solar cell performance are light absorption and hole mobility. Additionally, the interaction of the P3HT with PCBM, before and after annealing (which depends on the molecular weight and regioregularity), is also of critical importance for the composite films.

The most commonly used P3HT for BHJ solar cells is the electronic grade P3HT produced by Rieke Metals, which contains a minimum of residual catalyst or other metal impurities that may affect solar cell performance. This polymer is found to have an RR value of 90–93% and a molecular weight M_n of about 30 kDa, with a polydispersity (PDI) of approximately 2 (as determined by size exclusion chromatography, SEC).[68] Assuming the same level of polymer purity, deviations in regioregularity or molecular weight from these values have definite consequences on the intrinsic properties of the polymer and its performance in devices. It has been observed that increasing the polymer regioregularity in pristine P3HT leads to: 1) a red-shift in the thin film absorption,[69] 2) an increase in the solid-state absorption coefficient,[70] and 3) an increase in the mobility of the charge carriers.[71]

The effect of polymer molecular weight on the solid-state absorption of light is pronounced, as studied by Zen et al.[72] These authors showed that four P3HT samples with M_n values varying from 2.2 to 19 kDa (PDI = 1.2–1.5) had visibly different optical properties. The lowest molecular weight polymer gave a yellow film (even after annealing) with an absorbance maximum (λ_{max}) at 450 nm, while the 19-kDa sample produced a violet film with $\lambda_{max} = 555$ nm. In contrast, only a minor shift in the λ_{max} value is observed in solution. The pronounced red-shift in the solid-state spectrum of the high-molecular weight sample is suggested to be a consequence of the more effective packing of chains. This result is supported by FET mobility data, which show a three orders of magnitude increase in hole mobility in the annealed films as the molecular weight is increased from 2.2 kDa to 19 kDa.

Kline et al.[73] observed a similar effect for highly regioregular samples (RR > 98%) of P3HT with molecular weights (M_n) varying from 4 to 30 kDa. However, according to this study, both the high- and low-molecular-weight P3HT are capable of generating highly ordered films with coherent π–π stacked structures. The blue-shift in the absorbance of the polymer with lower molecular weight is proposed to be due to nonsaturated electronic properties at such low molecular weight, rather than chain twisting and disordering. Furthermore, a grain boundary model was proposed, in which the lower molecular weight polymers assemble into crystalline nanorods that pack in a random fashion and generate grain boundaries unfavorable for charge transport. At higher molecular weights, however, it is suggested that a truly semicrystalline polymer is formed, in which chain connectivity between crystalline domains is efficacious for charge transport through the polymer. With either of these views of the nanostructure within the polymer films, it is clear that higher molecular weight and higher regioregularity result in polymers that absorb more light and transport charges more efficiently.

The effect of molecular weight and regioregularity has also been investigated in films made from P3HT/PCBM blends. In a detailed study, Schilinsky et al.[74] found a dramatic effect of the P3HT molecular weight on the performance of the solar cell. Five samples of P3HT with M_n values varying from 2.2 to 19 kDa (PDI = 1.2–1.9) and equivalently high RR values were compared in 1:1 blends with PCBM. Samples with molecular weights less than 10 kDa give significantly blue-shifted absorption spectra and weak absorption across the visible spectrum that combine with significantly lower hole mobilities to give devices with efficiencies of less than 0.5%. Polymers with molecular weights greater than 10 kDa show efficiencies of 2–3% and EQE values of greater than 40% that extend from 400–650 nm. This finding suggests that P3HT with a molecular weight of less than 10 kDa does not have the ability to effectively harvest photons and transport charge. This finding is consistent with the results presented for pristine P3HT films discussed above. The effect of molecular-weight variations at higher molecular weights (20–50 kDa) has not been examined.

While the effect of the molecular weight of P3HT on both the optical and charge transport properties was found to be consistent for both pristine films and 1:1 blend films with PCBM, the effect of the regioregularity on device performance is still the object of some controversy. Considering the properties of the pristine P3HT films, it might be reasonable to speculate that the highest regioregularity would translate into the best photovoltaic performance because of the highly crystalline nature attainable for polymers with very high RR values, their commensurately high hole mobility, and their favorable absorption characteristics.

In the first study on the effect of P3HT regioregularity by Kim et al.,[70] this proposal was upheld. The solar cell performance was compared for three samples of P3HT with RR values of 90.7, 93, and 95.2%. Devices formed from 1:1 blends of these polymers with PCBM and annealed for two hours at 140 °C were found to give efficiencies of 0.7, 1.8, and 2.4%, respectively, under AM1.5 conditions. It should be noted that the M_n values for the three samples were 23.7, 17.8, and 14.2 kDa, respectively. It should also be noted that in the same study a P3HT sample with an RR value of 95.4% and a M_n value of 11.6 kDa was reported to give an efficiency of 4.4% in a 1:1 blend with PCBM after further optimization. These results suggest that increasing the regioregularity of the polymer leads to an improved device performance. Since only the P3HT sample with the highest measured RR value was subjected to extensive optimization, it would be instructive to see the effect of extensive optimization for the polymers with

lower RR values. This is especially true in light of the earlier results of Ma et al.,[3] who showed that the efficiency for a blend device consisting of a 1:0.8 blend of P3HT and PCBM increased from 0.82% to about 5% after annealing for 1 h at 150°C. The polymer used in this study (obtained from Rieke metals) had RR ≈ 90–93% and $M_n \approx 30$ kDa.

If it is assumed that molecular weight is not responsible for differences in performance, it is surprising that the P3HT sample with an RR value of 90–93% studied by Ma et al. was able to out-perform so dramatically the P3HT samples with RR values of 90.7% and 93% studied by Kim et al. In both studies the P3HT/PCBM blends were spin-coated from chlorobenzene, although significantly different concentrations were used (Kim: 60 mg mL^{-1}, Ma: 18 mg mL^{-1}) and the two blends had different compositions (1:1 and 1:0.8, respectively). While the results presented by Kim et al. seem to definitely suggest that a higher RR value gives better BHJ solar cells with PCBM, in light of the results of Ma et al. and considering the lack of a complete solar cell optimization for each RR sample, it appears that the extent to which small changes in the RR value can affect device performance is still in need of more conclusive proof.

The conclusion that maximizing the RR value of the P3HT component is ultimately beneficial was also called into question by a recent study by Sivula et al.[68] In this study the effect of the RR value on the thermal stability of the P3HT/PCBM solar cells was examined. A P3HT sample with an RR value of 96% and $M_n = 28$ kDa and a modified P3HT with an effective RR value of 91% and $M_n = 22$ kDa were compared. The modified P3HT is a random copolymer of 96% 3-hexylthiophene and 4% 3,4-dihexylthiophene. The incorporation of a small amount of the 3,4-dihexyl monomer induces a controlled amount of head-to-head linkages that lead to an effective lowering of the regioregularity of the P3HT. In this case, both polymers were observed to give energy conversion efficiencies of more than 4% (4.3% for the 96% RR sample and 4.4% for the 91% RR sample). While it must be taken into account that the sample with an RR value of 91% is a copolymer of unknown sequence distribution, these results (coupled with the results of Ma et al.) do suggest that maximizing the regioregularity of P3HT is not definitively necessary or ultimately beneficial. Furthermore, the role of polydispersity is unknown.

One important result that stems from the work of Sivula et al.,[68] is the finding that the thermal stability of the BHJ composite layer depends on the RR value of the polymer. It was shown in the comparison of the samples with RR values of 96% and 91% that a nanoscale phase-separated film morphology is retained in the sample with the lower RR value after 30 minutes of annealing at 150°C, while micrometer-sized aggregates of PCBM are observed for the P3HT blend with an RR value of 96% under the same conditions. The thermal stability of the morphology and device performance reported by Sivula et al. for the sample with an RR value of 91% is consistent with the results presented by Ma et al. for the P3HT sample with an RR value of 90–93%. At this time, it is clear that further detailed studies on the effect of the regioregularity of the polymer are required.

For comparison purposes, the best reported P3HT/PCBM (1.0:0.8) devices show an energy conversion efficiency of about 5%, $V_{oc} = 0.63$ V, $J_{sc} = 9.5$ mA cm^{-2}, and FF = 0.68. One will notice that the V_{oc} value is smaller than that for MDMO-PPV/PCBM cells, as is expected based on the HOMO–LUMO difference between the donor and the acceptor (Figure 2). Most notably, the current density in the P3HT/PCBM devices is nearly twice that of the MDMO-PPV/PCBM devices. This is primarily a reflection of the enhanced absorption of light, because of the broader absorption spectra and the greater amount of polymer present in the P3HT devices relative to that in the MDMO-PPV devices.

Another important factor to consider is the mobility of the charge carriers in these optimized blends. For pristine MDMO-PPV, the hole mobility measured in an SCL sense (using a diode configuration to best represent charge transport in a solar cell) is on the order of 10^{-7} cm^2 V^{-1} s^{-1}.[75] However, blending with PCBM at the optimal ratio of 1:4 results in the hole mobility increasing to 10^{-4} cm^2 V^{-1} s^{-1}. This strong increase in the mobility of the charge carriers on blending with PCBM certainly reflects a morphological component. Pristine films of MDMO-PPV have been shown to exhibit a disordered morphology, with the polymer chains exhibiting coiled ringlike conformations.[76] It is suspected that the significantly higher hole mobilities measured in the percolated blends are due to the influence of the large weight fraction of PCBM, which could force the MDMO-PPV into a more favorable conformation for efficient packing and interchain charge transport.

The morphological influence on hole mobility is clear when it is considered that hole mobility does not increase further for weight percentages of PCBM greater than 67% in MDMO-PPV blends.[77] This weight fraction corresponds to the threshold above which pure PCBM domains exist in a continuous matrix of 1:1 MDMO-PPV/PCBM.[78] This finding supports the notion that maximizing the amount of PCBM in close contact with MDMO-PPV can help to maximize the ability of the polymer to conduct charge. In contrast, SCL mobilities of 10^{-4} cm^2 V^{-1} s^{-1} are typically measured for pristine P3HT, and very similar values can be achieved in annealed blends of P3HT and PCBM.[65] This result points to the fact that the morphological role in controlling the hole mobility in P3HT devices is based solely on the ability of the polymer to reorganize into an effective charge-transporting phase. The electron mobility in both P3HT and MDMO-PPV blends is on the order of 10^{-3} cm^2 V^{-1} s^{-1}, which is on the same order as that measured for pristine PCBM under the same conditions. The role that unbalanced electron and hole transport can play in device operation will be described in the following section.

In concluding this section on polymer morphology, it may be stated that attaining a desirable morphology in polymer–fullerene composite solar cells is critical for device performance. In the design of new polymers (or fullerenes) for BHJ solar cells, it is clear that optimizing only the electronic structure is not sufficient. It is essential to consider whether or not processing of the material can be carried out to give a final composite structure with an effective morphology.

5. Considerations for the Optimization of Polymer–Fullerene BHJ Solar Cells

In the previous two sections the importance of optimizing the electronic structure of both the donor and the acceptor as well as the morphology of the composite was discussed. While the best currently available devices are composed of P3HT/PCBM and MDMO-PPV/PCBM composites, much effort is being devoted to enhancing the efficiency of BHJ solar cells by developing a deeper understanding of the processes and interactions that dominate the performance of solar cells and developing new materials that are more effective for device operation. In the following sections, several key areas that have been examined in an attempt to improve solar energy conversion will be discussed along with key concepts that ought to be considered in the search for high efficiency.

5.1. New Materials

The prototypical BHJ solar cells based on MDMO-PPV/PCBM and P3HT/PCBM composites discussed above show the extent of optimization that is required to generate efficient polymer–fullerene solar cells. However, a variety of other approaches have been used in attempts to overcome some of the inherent limitations of these typical examples. These limitations can largely be gleaned directly by a consideration of the fundamental mechanism for photoconversion in these excitonic solar cells (Scheme 1), which begins with light absorption.

The photon flux reaching the surface of the earth from the sun occurs at a maximum of approximately 1.8 eV (700 nm); however, neither MDMO-PPV ($E_g = 2.2$ eV) nor P3HT ($E_g = 1.9$ eV) can effectively harvest photons from the solar spectrum. It is calculated that P3HT is only capable of absorbing about 46 % of the available solar photons[31] and only in the wavelength range between 350 nm and 650 nm. The limitation in the absorption is primarily due to limited spectral breadth rather than the absorption coefficient, as conjugated polymers typically have extremely high absorption coefficients on the order of 10^5 cm^{-1}.[79] Developing a polymer that could capture all of the solar photons down to 1.1 eV would allow absorption of 77 % of all the solar photons.[21] Expanding the spectral breadth of absorption in polymer–fullerene composites has most commonly been pursued by extending (or shifting) the polymer absorption spectrum into the near-infrared region. This is primarily achieved through the use of low-bandgap polymers, which has led to efficiencies as high as 3.5 %[31] in polymer–fullerene composite solar cells. While low-bandgap polymers have often been touted as the solution of this problem, merely having a lower energy onset for absorption is not sufficient to harvest more solar photons. What is needed is to extend the overlap with the solar spectrum to gain broader coverage while also retaining high absorption coefficients at relevant wavelengths and suitable energy levels for interaction with PCBM.

A first approach towards these goals focused on broadening the absorption of known polymers through the UV and visible regions. An excellent example is afforded by poly(3-vinylthiophenes), such as **1**.[80] The incorporation of chromophores that are conjugated to the backbone through the 3-vinyl linkage leads to a broadening of the wavelengths at which high photoconversion efficiencies can be achieved. In a direct comparison with P3HT/PCBM devices, cells with polymer **1** afforded 3.2 % efficiency versus 2.4 % with P3HT under the same conditions. The enhanced performance of polymer **1** can be attributed to the increased photocurrent in the 400–500 nm range. It is interesting to note that despite its irregular structure, copolymer **1** is able to afford highly efficient solar cells when blended with PCBM in a 1:1 ratio. Other examples of poly(3-vinylthiophenes) have also been reported to achieve efficiencies greater than 1 %.[81]

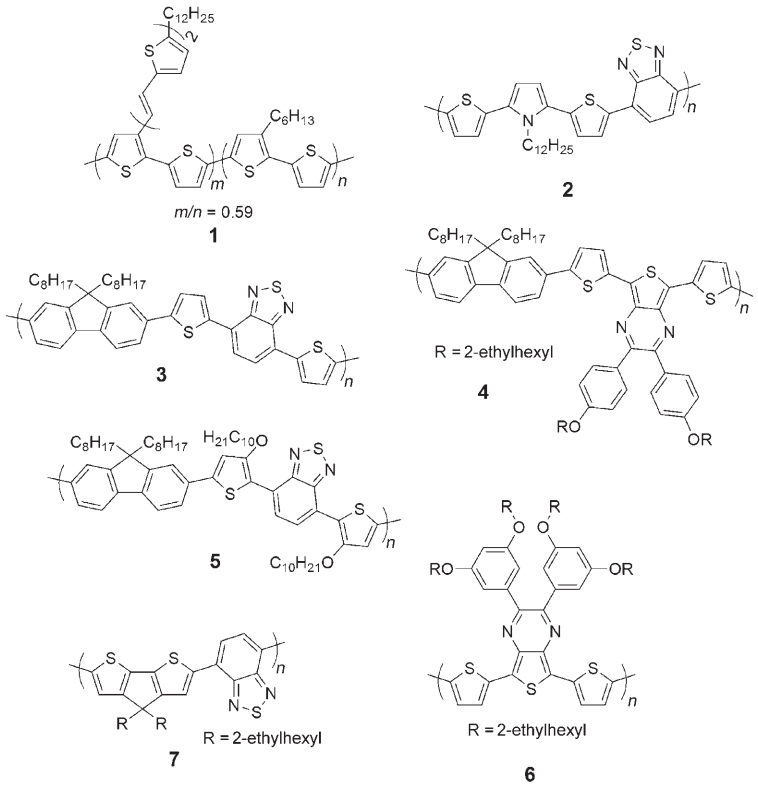

The second and most common approach to increasing the spectral breadth of absorbed photons is the use of so-called low-bandgap polymers,[82] which are loosely defined as polymers with a bandgap less than 1.5 eV. However, in terms of polymer-based photovoltaic systems, any polymer with a bandgap less than that of P3HT (that is, < 1.9 eV) is often referred to as a low-bandgap polymer. In several cases efficiencies in the range of 1 to 3.5 % have been achieved. Compounds **2**–**7** represent a few of the more successful polymers employed to-date. The most common synthetic

technique used to achieve low-bandgap polymers is the donor–acceptor approach, in which alternating electron-rich and electron-poor units define the polymer backbone.[83] The best examples of this class reported thus far are based almost exclusively on benzothiadiazole (or analogues) as the acceptor in combination with several different donor groups.

Polymer **2**, poly[{*N*-dodecyl-2,5-bis(2-thienyl)pyrrole}-*alt*-{2,1,3-benzothiadiazole}] (PTPTB), is capable of an efficiency of about 1% when blended with PCBM in a 1:3 ratio.[28] The low bandgap (ca. 1.6 eV) of PTPTB is effective for extending the photocurrent in these devices out to nearly 800 nm and giving a broad coverage across much of the visible region. However, 70 nm thick films of the 1:3 blends with PCBM afford peak EQE values of only about 20% as barely 40% of the available photons are absorbed at the λ_{max} value of 550 nm.

Another class of polymers are the APFO polymers (such as **3**, a poly[{2,7-(9,9-dialkylfluorene)}-*alt*-{5,5-(4,7-di-2′-thienyl-2,1,3-benzothiadiazole)}], which are reported to afford efficiencies as high as 2.8%[84] and EQE values greater then 50% in the 350–600 nm region in 1:3 or 1:4 blends with PCBM.[85]. However, the high performance of these APFO polymers cannot be attributed primarily to an increase in the absorption, as the bandgap of **3** is only about 1.9 eV while the V_{oc} values are on the order of 1 V. Further variations of this structure have been explored and the introduction of the much stronger acceptor thienopyrazine has lowered the bandgap to 1.6 eV in APFO-Green 5 (**4**).[86] In this case, efficiencies up to 2.2% were measured in 1:3 blends with PCBM at a film thickness of 140 nm. Here, EQE values as high as 40% were measured at 700 nm, the wavelength at which the photon flux from the sun is a maximum, while open circuit voltages are reduced to 0.6 V from the 1.0 V with the APFO polymers described above. However, the high currents (9 mA cm^{-2}) and respectable fill factors (0.4–0.5) suggest an effective low-bandgap polymer.

A closely related polymer **5** also afforded efficiencies of 1.6% in 1:4 blends with PCBM.[87] The lower bandgap of **5** (1.78 eV) relative to **3** is due to the stronger donor–acceptor interaction resulting from the use of the electron-rich 3-alkoxythiophene units. Another thienopyrazine-based polymer (**6**) has also been reported to give an efficiency of about 1.1% with a bandgap of 1.2 eV.[88] To our knowledge, this is the lowest bandgap polymer reported to date that affords an efficiency of more than 1%. Photocurrent production is demonstrated up to 1000 nm and V_{oc} values of 0.56 V are observed in 1:4 blends with PCBM. The important point of this study is that by carefully engineering the band energies of the polymer the authors were able to effect a 0.7 eV reduction in the bandgap relative to P3HT while only reducing the V_{oc} value by about 0.05 V. Success was achieved because the measured LUMO–LUMO difference was 0.45 eV and the measured (donor-HOMO)–(acceptor-LUMO) difference was 1.01 eV, based on an electrochemical bandgap of 1.46 eV (optical energy gap $E_g = 1.2$ eV).

To date, the most efficient example of a low-bandgap polymer for use in solar cells is poly[{2,6-(4,4-bis(2-ethylhexyl)-4*H*-cyclopenta[2,1-*b*;3,4-*b*′]dithiophene}-*alt*-{4,7-(2,1,3-benzothiadiazole)}] (**7**).[89] This polymer has a measured optical bandgap of about 1.45 eV, and in a 1:1 blend with PCBM shows a power conversion efficiency of 2.7% and a V_{oc} value of 0.65 V, with a peak EQE value of about 30% and photocurrent production at wavelengths longer than 900 nm. The excellent performance of **7** can be attributed to a broad absorption spectrum and high mobility of the charge carriers (2×10^{-2} cm^2 V^{-1} s^{-1} in FETs). The ability to achieve efficiencies approaching 3% in a 1:1 blend with PCBM correlates with the superior miscibility of **7** with PCBM relative to other donor–acceptor polymers. The use of the C_{70} derivative of PCBM (C_{70}-PCBM or [70]PCBM) with **7** lead to efficiencies as high as 3.5%.[31,89] The main reason for this increase in performance is the much greater absorption of C_{70} in the visible region relative to that of C_{60}. The high symmetry of C_{60} renders low-energy transitions formally dipole forbidden, thereby resulting in a very weak absorption of light in the visible region, despite the bandgap of 1.8 eV.

In contrast, C_{70} has an unsymmetrical structure with significantly stronger absorption across the visible region.[90] In fact, the measured extinction coefficient of [70]PCBM is nearly five time that of [60]PCBM at 600 nm and nearly 20 times higher at 475 nm.[91] As a result, [70]PCBM has been used to improve the performance of a variety of polymer solar cells, following the initial report that MDMO-PPV/[70]PCBM devices are capable of energy conversion efficiencies of 3.0% with significantly improved short-circuit current densities and external quantum efficiencies relative to [60]PCBM analogues, primarily as a result of the improved photon harvesting.[90] It should be noted that the best efficiencies with MDMO-PPV/[70]PCBM were achieved with a ratio of 4.6:1, whereas in the case of [60]PCBM the optimum efficiency was obtained at a 4:1 ratio. This finding is a reflection of the poorer miscibility of [70]PCBM with MDMO-PPV, which is in accord with the overall lower solubility observed with derivatives of the higher fullerene.

Several other examples of the use of [70]PCBM and other soluble C_{70} derivatives have been reported, primarily in combination with low-bandgap polymers as an effort to absorb light at the high-energy end of the visible spectrum, which is not achievable with most low-bandgap polymers.[92–94] In this case efficiencies as high as 2.4% in 1:4 blends of polymer **5** with [70]PCBM were found, an improvement over the 1.6% described earlier with [60]PCBM. This improved efficiency is attributed primarily to significantly higher EQE values measured in the wavelength range 350–600 nm. An extension of the above system to the C_{84} derivative ([84]PCBM) has led to a significantly reduced performance of the solar cell despite the even stronger absorption of [84]PCBM in the visible region; this problem is likely directly related to the very poor solubility of [84]PCBM.[91]

Overall, it is clear that strategies that focus on optimizing both the polymer and the fullerene structures can afford significant improvement in the ability to harvest light across a broader spectral range. Device efficiencies with these novel materials have now reached 3.5% and, with the same level of morphological optimization as expended on P3HT blends with PCBM, efficiencies exceeding 5% are predicted. A key point with low-bandgap polymers is the need not only for broadened absorption spectra, but also high absorption

coefficients of the thin film, high mobilities, and effective physical and electronic interactions with the fullerene components.

In addition to higher fullerenes, a variety of soluble C_{60} derivatives have been synthesized (**8**–**10**) and employed in BHJ solar cells with varying success. The focus in this case was

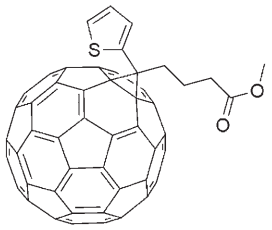

8

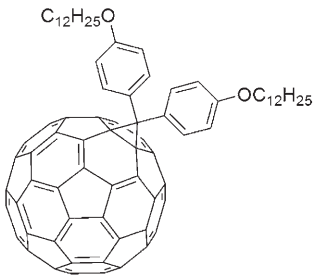

9

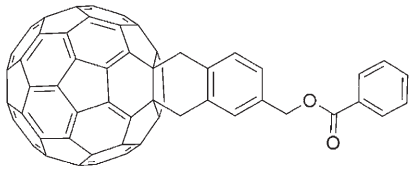

10

not to increase the absorption of visible light, but rather to improve miscibility, the mobility of the charge carriers, and other aspects of performance that are influenced by the structure of the soluble fullerene employed. A further motivation for testing new soluble C_{60} derivatives is the development of a fundamental structure–property relationship and a guiding design principle for improving the performance of the solar cells through the use of the optimized fullerene acceptors. As mentioned earlier, substitution of the fullerene with a variety of solubilizing groups has only led to small changes in the electronic structure. Therefore, the focus has been to optimize the solubilizing group to develop the right level of miscibility with the specific polymeric donor employed, such that an "ideal" morphology will be thermodynamically favorable or at least can be easily trapped kinetically.

The concept of generating specific fullerenes that are compatible with specific polymers has great potential for increasing the performance of solar cells through the optimization of the morphology. In the simplest study, a series of PCBM derivatives in which the nature of the alkyl ester was varied (methyl to hexadecyl) were synthesized and tested in solar cells.[95] While the solubility of the fullerene derivatives increased with increasing alkyl chain length, the performance in MEH-PPV (poly[2-methoxy-5-(2-ethylhexyl)-1,4-phenylene]-*alt*-(vinylene)) composite solar cells reached a maximum with the butyl ester derivative. The initial increase in the performance with an increase in the size of the alkyl group was attributed to the greater miscibility of the fullerene with MEH-PPV. However, alkyl chains longer than butyl resulted in decreased solar cell performance probably because of a decrease in the mobility of the charge carriers in the fullerene phase as a result of the longer alkyl chains.

Other variations of the PCBM structure have also been examined. For example, the recently reported thienyl analogue of PCBM[96] (ThCBM, **8**) has demonstrated efficiencies as high as 3.0% in 1:1 blends with P3HT. A wide variety of other PCBM analogues have recently been reported, but no distinct advantage over PCBM has been illustrated.[25] Efforts to significantly alter the structure of the solubilizing group on the fullerene have generally led to a decrease in the performance of the solar cell. One interesting case is the diphenylfullerene DPM-12 (**9**),[97] which is significantly more soluble than PCBM and proves to be more miscible with MDMO-PPV and P3HT. The enhanced miscibility of **9** appears to result in a higher level of recombination, as a consequence of the less well-defined phases for effective charge transport. This aspect, combined with an electron mobility 40 times lower than PCBM, results in decreased performance. Only one class of soluble fullerenes has thus far been reported to give performance commensurate to that of PCBM, and those are the dihydronaphthylfullerenes such as **10**.[67] In a test series, the electronic structure of the terminal benzene ring was varied from trimethoxy to perfluoro. The simple benzoate derivative **10** gave the best performance with (un-optimized) efficiencies of 4.5% reported in P3HT solar cells at a polymer/fullerene ratio of 1:0.82, whereas P3HT/PCBM devices prepared in a parallel study showed 4.4% efficiency at an optimal ratio of 1:0.67.

5.2. Conceptual and Mechanistic Optimization

Another mechanistic factor in need of optimization is the exciton diffusion length of the polymer. In the polymer–fullerene composite solar cells with the most well-defined and optimized morphologies, the exciton diffusion length should not be a limiting factor in device performance because of the intimate mixing of the polymer and fullerene phases. However, the exciton diffusion length remains an issue with most polymer–fullerene BHJ solar cells. A variety of different routes have been suggested to increase the exciton diffusion length in the polymer.

The first approach, discussed in Section 3, relies on resonance energy transfer to effectively enhance the exciton diffusion length. An alternative approach attempts to use triplet excitons rather than singlet excitons. Triplet excitons are advantageous because of their significantly longer lifetimes relative to singlet excitons (10^{-6} s versus 10^{-9} s). Since the exciton diffusion length depends both on the mobility and lifetime of the exciton, an increase in the lifetime could translate into an increased exciton diffusion length. While this approach has been suggested and examined for use in bilayer cells,[98] it has never been specifically exploited in polymer–fullerene BHJ solar cells. It should also be noted that photocurrent generation in typical C_{60}-based bilayer devices is dominated by triplet excitons.[11]

Another consequence of using triplet excitons as the primary excited species of the donor, is the greatly reduced

likelihood of geminate recombination. The triplet exciton approach has recently been used by Guo et al.[99] They used a platinumacetylide polymer that provides for efficient heavy-atom-induced intersystem crossing ($K_{isc} > 10^{11}\,s^{-1}$), which leads to the exclusive generation of triplet excitons in the polymer. When the polymer was blended in a 1:4 ratio with PCBM, device efficiencies of about 0.25% were achieved, despite the poor spectral overlap of the polymer with the solar spectrum. The photovoltaic performance was attributed to the fact that the charge-separated state of the donor–acceptor pair was sufficiently lower in energy than the triplet state of the donor polymer to favor charge separation after excitation. Most importantly, the geminate pair that formed after charge transfer and prior to the generation of free charges was spin correlated to the triplet state and thus governed by a spin-forbidden, direct back electron transfer, which prohibits geminate recombination. This situation is in sharp contrast to that for singlet excitons where spin-allowed geminate recombination is effective in organic materials with low dielectric constants as a result of the strong coulombic binding energy of the geminate electron–hole pair.

Three main processes must be considered from the time an exciton at the donor–acceptor interface generates a geminate electron–hole pair, to the time when charges are collected at the electrodes: geminate recombination, bimolecular recombination, and charge transport. These parameters are related to the efficiency of collecting formed charges. It is estimated that in the case of MDMO-PPV only 60% of the formed geminate pairs are dissociated and contribute to the short-circuit current.[100] The geminate pairs can either recombine or separate into free charges, with each process being characterized by its own relative rate and with the rate of separation into free charges being dependent on the electric field.

The fact that only 60% of geminate pairs dissociate under short-circuit conditions is a major loss mechanism in MDMO-PPV/PCBM solar cells. Interestingly, the dissociation efficiency of geminate pairs is dependent on the composition of the blends, specifically on the PCBM content.[77] At the optimal 4:1 ratio (80 wt% PCBM), 60% of the geminate pairs can be separated and collected. Reducing the fullerene content to 67% results in a decrease in the efficiency of the charge separation to about 37%. This decrease is due primarily to the decreased dielectric constant in the film with lower fullerene content, as a higher dielectric constant helps to drive the electron–hole separation. For P3HT/PCBM blends, the situation is somewhat different, and 90% of the geminate pairs are estimated to be effectively dissociated under short-circuit conditions in annealed blends.[65] This situation contributes to the superior performance of P3HT/PCBM devices. The reason for the enhancement in charge separation efficiency with P3HT is attributed to the geminate pair having a longer lifetime and a larger mean separation of charges. Therefore, although the mobilities of the charge carriers in P3HT/PCBM and MDMO-PPV/PCBM solar cells are very similar and the PPV system gives a higher V_{oc} value, the improved charge-separation efficiency coupled with the enhanced absorption of light lead to improved performance in P3HT devices.

Bimolecular recombination is also a concern in these BHJ devices. In these composites, the notion that free, oppositely charged species would meet and recombine at an interface is easily accepted. The initial product of bimolecular recombination is a geminate pair, which can re-dissociate on the basis of the factors described above. Therefore, not all bimolecular recombination events contribute to a loss mechanism. The problem of bimolecular recombination in polymer–fullerene BHJ solar cells has been investigated by Koster et al.[101] The rate of bimolecular recombination in these cells is determined by the phase with the lowest charge-carrier mobility. Conceptually, this is due to the fact that the fastest carrier (electrons in the case of P3HT and MDMO-PPV composites with PCBM) cannot cross the phase interface and must wait for the slowest carrier to recombine.[102]

The importance of bimolecular recombination is thus related to the mobilities of the charge carriers in the two phases. In short, increasing the carrier mobilities results in both increased extraction of the charge carriers and increased bimolecular recombination. Therefore, developing the optimum mobilities of the charge carriers in the two phases and an optimal balance between the two is necessary. A recent study,[102] has sought to derive this relationship. For both MDMO-PPV/PCBM and P3HT/PCBM systems, the electron mobility μ_e and hole mobility μ_h were measured to be 10^{-3} and $10^{-4}\,cm^2\,V^{-1}\,s^{-1}$, respectively. It is estimated that in the optimal case the mobilities will be balanced and range from 10^{-1} to $1\,cm^2\,V^{-1}\,s^{-1}$. If the mobilities are on the order of $\mu_e = 10^{-6}$ and $\mu_h = 10^{-7}\,cm^2\,V^{-1}\,s^{-1}$, 45% of carriers should recombine through bimolecular recombination, under the conditions assumed for deriving these relationships. In a case where $\mu_e = 10^{-1}$ and $\mu_h = 10^{-2}\,cm^2\,V^{-1}\,s^{-1}$, only 0.38% of carriers should recombine. Increasing the mobilities further is thought to have a negative effect because of an induced decrease in the V_{oc} value at very high mobilities ($10^7\,cm^2\,V^{-1}\,s^{-1}$).

Balanced mobilities of the charge carriers are needed to avoid the build-up of space charge in the devices. It has been demonstrated that photocurrent reaches the fundamental space–charge limit when the electron and hole mobilities differ by more that two orders of magnitude.[103] The build-up of space charge as well as high levels of bimolecular recombination have a strong effect on reducing the fill factor in solar cells.[101] Therefore, to maximize the efficiency of the soalr cell through reduction of bimolecular recombination, the elimination of space charge and the maximum effective extraction of charge-carrier mobilities must be balanced and optimized.

Another aspect of optimization that could lead to the enhancement of solar cell performance is the minimization of wasted energy. This is best done by considering the band structures of P3HT and PCBM. The LUMO–LUMO difference of the two materials is about 1 eV, whereas it is generally accepted that as little as 0.3–0.4 eV is necessary and sufficient for effective charge transfer (see discussion in Section 3). As a consequence, 0.6–0.7 eV are "wasted" and are not reflected in the V_{oc} value of the device. Therefore, a donor–acceptor pair that displays suitable band differences to minimize wasted energy and maximize the V_{oc} value should be sought, while

retaining a donor bandgap that is effective for harvesting the solar spectrum, as described in Section 5.1.

Two approaches can be used to achieve this goal: the band structure of the polymer can be modified to better match that of the fullerene, or the energy levels of the fullerene can be tuned to better match the polymer. The simpler route attempts to lower simultaneously both the LUMO and HOMO of the polymer structure. Several examples have already been discussed in Section 5.1. in regard to low-bandgap polymers. These rely primarily on the incorporation of electron-poor units into the polymer backbone to increase the electron affinity of the polymer and thus lower the LUMO. The incorporation of such electron-poor units often leads to a concomitant decrease in the HOMO energy of the polymer in such donor–acceptor systems.[35] However, it should not be assumed that a donor–acceptor method is the only synthetic design strategy or even necessarily the most effective for pursuing such targets, as such donor–acceptor copolymers often suffer from low absorption coefficients.

5.3. Stability of the Solar Cells

A final concern of critical relevance to the optimization of polymer–fullerene BHJ solar cells is the stability of the devices. Stability can be assessed in regard to a variety of different parameters including, in particular, ambient and thermal stability. While ambient stability may be realized through encapsulation to protect devices from the action of oxygen and water, thermal stability is a critical issue that currently plagues organic BHJ solar cells. It is well-documented that the phase-instability of MDMO-PPV/PCBM solar cells renders them unstable to long-term exposure to elevated temperatures.[48] Devices based on P3HT/PCBM show better thermal stability because of the inherently greater miscibility of the two components. The precise primary structure of the P3HT has been proposed to play a major role in the thermal stability of the composite (see discussion in Section 4).[68] Polymer samples with regioregularities greater than 96% phase segregate from PCBM much more readily than samples with RR values of 91–93%. It is expected that a stronger driving force for crystallization in the more regioregular samples enhances phase segregation with PCBM. Thus, it is expected that the precise primary structure of any polymer used in a fullerene BHJ cell will have a strong effect not only on the performance, but also on the stability of the device.

Two general routes have been explored to improve the thermal stability of polymer–fullerene BHJ solar cells and reduce phase separation: the use of compatibilizers and cross-linking. The use of additive compatibilizers in the form of diblock copolymers functionalized with P3HT grafts on one block and fullerene grafts on the other block have resulted in the generation of homogenous composites, which display enhanced thermal stability.[104] When 17 wt% of the diblock copolymer is added to a 1:1 blend of P3HT and PCBM, the efficiencies of the solar cells remain constant at about 2.5% even after 10 h of annealing at 140 °C. For comparison, a 1:1 P3HT/PCBM device measured under the same conditions shows an efficiency of only about 1.2% after 10 h of annealing. As discussed in Section 4, TEM imaging provided a correlation between the performance of the solar cells and thermally driven phase segregation.

The use of cross-linkable moieties on the polymer and/or the fullerene has also been proposed as a means to enhance the phase stability of the BHJ solar cells. In the best example of this strategy, an epoxide-functionalized PCBM was used as a cross-linkable fullerene derivative.[105] In this case, cross-linking of the fullerenes was achieved either by strictly thermal treatment at 140 °C or by thermal treatment in the presence of a small amount of chemical initiator. When directly compared to P3HT/PCBM (1:2 by weight) blend films, analogous blends of P3HT and the cross-linkable fullerene showed significantly improved phase stability, to the extent that no phase separation was observed even on extended annealing. The real benefit here is that when the fullerenes are effectively polymerized within the composite film, their diffusion is no longer a factor even above the T_g value of the polymer. After extended thermal annealing, however, device performance was observed to decrease through an unknown degradation mechanism. A similar approach has also been pursued with a butadiyne-substituted fullerene.[106] The use of cross-linkable polythiophenes has also been explored and several polythiophenes bearing cross-linkable moieties have been synthesized.[107]

A possible drawback to the use of cross-linkable polymers was discovered in the study of Murray et al. on cross-linkable regioregular polythiophenes.[108] Cross-linking of the polymer films results in a blue-shift in the polymer absorption spectra, which can be directly correlated with the density of cross-linking in the polymer. It is proposed that cross-linking at high temperature causes a more disordered morphology to be locked in and prevents the adoption of the favorable chain conformation and packing for the realization of the highly ordered polymer chains responsible for strong absorption of visible light and charge transport. Ultimately, such practical issues will have to be addressed more seriously if these devices are to find viable application.

6. Summary and Outlook

In the 12 years that have elapsed since the discovery of the polymer–fullerene BHJ solar cells, dramatic improvements in fundamental understanding, device construction, and processing of the active layer have led to efficiencies of about 5% being achieved by several research groups using blends of P3HT and PCBM. The major accomplishment has been the development of a much deeper understanding of the complex interplay between the electronic and physical interactions of the polymer and fullerene component and how this ultimately affects the device performance. The lessons learnt from the present generation of polymer–fullerene photovoltaic systems will surely assist in the design of the next generation of optimized organic solar cells.

The challenges for the next level of optimization have been delineated here and focus not only on cementing a much deeper level of mechanistic understanding of the processes

involved, but developing and optimizing new materials to capitalize on such new knowledge. The low-bandgap polymers discussed in Section 5 are one such example of how structural optimization of a polymer can lead to materials that can better absorb solar radiation, while retaining high voltages and charge-carrier mobilities. The complete optimization of such new materials has a long way to go, but the path paved by the optimization of P3HT/PCBM and MDMO-PPV/PCBM devices will certainly aid in this process. A great challenge that remains is the very practical challenge of long-term device stability, although efforts involving cross-linkers and compatibilizers may contribute to solving such issues. Another practical challenge is to move beyond the small-area devices used in a laboratory setting and to investigate how more realistic devices and processing conditions influence performance. Recent studies by Schilinsky et al. has shown that efficiencies of 4% can be achieved in devices based on P3HT and PCBM by using the reel-to-reel compatible technique of doctor blading, but that distinct differences exist between bladed and spin-coated devices.[109]

A number of new approaches are also being explored for the optimization of polymer–fullerene solar cells. The use of block copolymers in which one block contains pendant fullerenes has been suggested as one method to achieve greater control over the morphology in these BHJ devices.[104,110] Many other improvements have been sought, by modifying the architecture of the device as a whole, while retaining the essential nature of the BHJ active layer. Specifically, the use of a TiO_x layer inserted between a P3HT/PCBM composite layer and the Al electrode has been used as an optical spacer to increase the absorption of light in the active layer and has been shown to give considerable enhancement in the photocurrent generated across the visible spectrum (maximum EQE value ca. 90%).[111] The extent to which subtle changes in interfacial layers can influence device performance is very nicely illustrated by a recent study with P3HT/PCBM devices in which modification of the PEDOT-PSS layer by the addition of mannitol improved the performance of the device from 4.5 to 5.2% as a result of a decreased series resistance in the device.[53] Such results, coupled with the discussions in this Review, indicate that much room exists for improvement in polymer–fullerene BHJ solar cells at all levels of device construction and composition. The pursuit of such optimizations promises to be an informative and ultimately useful endeavor.

We acknowledge financial support of our research on photovoltaic systems by the U.S. Department of Energy, Basic Energy Sciences (no. DE-AC03-76SF00098). B.C.T. thanks the American Chemical Society Petroleum Research Fund for funding through the Alternative Energy Postdoctoral Fellowship.

Received: June 8, 2007

[1] B. A. Gregg, *J. Phys. Chem. B* **2003**, *107*, 4688–4698.
[2] C. W. Tang, *Appl. Phys. Lett.* **1986**, *48*, 183–184.
[3] W. Ma, C. Yang, X. Gong, K. Lee, A. J. Heeger, *Adv. Funct. Mater.* **2005**, *15*, 1617–1622.
[4] G. Li, V. Shrotriya, J. Huang, Y. Yao, T. Moriarty, K. Emery, Y. Yang, *Nat. Mater.* **2005**, *4*, 864–868.
[5] M. Reyes-Reyes, K. Kim, D. L. Carroll, *Appl. Phys. Lett.* **2005**, *87*, 083506.
[6] J. Xue, B. P. Rand, S. Uchida, S. R. Forrest, *J. Appl. Phys.* **2005**, *98*, 124903.
[7] J. Xue, B. P. Rand, S. Uchida, S. R. Forrest, *Adv. Mater.* **2005**, *17*, 66–71.
[8] J. Xue, S. Uchida, B. P. Rand, S. R. Forrest, *Appl. Phys. Lett.* **2004**, *84*, 3013–3015.
[9] N. S. Sariciftci, D. Braun, C. Zhang, V. I. Srdanov, A. J. Heeger, G. Stucky, F. Wudl, *Appl. Phys. Lett.* **1993**, *62*, 585–587.
[10] M. Granstrom, K. Petritsch, A. C. Arias, A. Lux, M. R. Andersson, R. H. Friend, *Nature* **1998**, *395*, 257–260.
[11] P. Peumans, A. Yakimov, S. R. Forrest, *J. Appl. Phys.* **2003**, *93*, 3693–3723.
[12] J. J. M. Halls, C. A. Walsh, N. C. Greenham, E. A. Marseglia, R. H. Friend, S. C. Moratti, A. B. Holmes, *Nature* **1995**, *376*, 498–500.
[13] G. Yu, A. J. Heeger, *J. Appl. Phys.* **1995**, *78*, 4510–4515.
[14] C. J. Brabec, N. S. Sariciftci, J. C. Hummelen, *Adv. Funct. Mater.* **2001**, *11*, 15–26.
[15] R. Koeppe, N. S. Sariciftci, *Photochem. Photobiol. Sci.* **2006**, *5*, 1122–1131.
[16] *Photoinduced Electron Transfer* (Eds.: M. A. Fox, M. Chanon), Elsevier, Amsterdam, **1988**.
[17] H. Hoppe, N. S. Sariciftci, *J. Mater. Res.* **2004**, *19*, 1924–1945.
[18] C. J. Brabec, A. Cravino, D. Meissner, N. S. Sariciftci, T. Fromherz, M. T. Rispens, L. Sanchez, J. C. Hummelen, *Adv. Funct. Mater.* **2001**, *11*, 374–380.
[19] A. Gadisa, M. Svensson, M. R. Andersson, O. Inganas, *Appl. Phys. Lett.* **2004**, *84*, 1609–1611.
[20] P.-M. Allemand, A. Koch, F. Wudl, *J. Am. Chem. Soc.* **1991**, *113*, 1050–1051.
[21] S. Gunes, H. Neugebauer, N. S. Sariciftci, *Chem. Rev.* **2007**, *107*, 1324–1338.
[22] T. B. Singh, N. Marjanovic, G. J. Matt, S. Gunes, N. S. Sariciftci, A. Montaigne Ramil, A. Andreev, H. Sitter, R. Schwodiauer, S. Bauer, *Org. Electron.* **2005**, *6*, 105–110.
[23] M. T. Rispens, A. Meetsma, R. Rittberger, C. J. Brabec, N. S. Sariciftci, J. C. Hummelen, *Chem. Commun.* **2003**, 2116–2118.
[24] M. Keshavarz-K, B. Knight, R. C. Haddon, F. Wudl, *Tetrahedron* **1996**, *52*, 5149–5159.
[25] F. B. Kooistra, J. Knoll, F. Kastenberg, L. M. Popescu, W. J. H. Verhees, J. M. Kroon, J. C. Hummelen, *Org. Lett.* **2007**, *9*, 551–554.
[26] V. I. Arkhipov, H. Bassler, *Phys. Status Solidi A* **2004**, *201*, 1152–1187.
[27] G. L. Gaines, M. P. O'Neil, W. A. Svec, M. P. Niemczyk, M. R. Wasielewski, *J. Am. Chem. Soc.* **1991**, *113*, 719–721.
[28] C. J. Brabec, C. Winder, N. S. Sariciftci, J. C. Hummelen, A. Dhanabalan, P. A. van Hal, R. A. J. Janssen, *Adv. Funct. Mater.* **2002**, *12*, 709–712.
[29] C. Winder, G. Matt, J. C. Hummelen, R. A. J. Janssen, N. S. Sariciftci, C. J. Brabec, *Thin Solid Films* **2002**, *403–404*, 373–379.
[30] L. J. A. Koster, V. D. Mihailetchi, P. W. M. Blom, *Appl. Phys. Lett.* **2006**, *88*, 093511.
[31] C. Soci, I.-W. Hwang, D. Moses, Z. Zhu, D. Waller, R. Guadiana, C. J. Brabec, A. J. Heeger, *Adv. Funct. Mater.* **2007**, *17*, 632–636.
[32] M. C. Scharber, D. Muhlbacher, M. Koppe, P. Denk, C. Waldauf, A. J. Heeger, C. J. Brabec, *Adv. Funct. Mater.* **2006**, *18*, 789–794.

[33] V. D. Mihailetchi, J. K. J. van Duren, P. W. M. Blom, J. C. Hummelen, R. A. J. Janssen, J. M. Kroon, M. T. Rispens, W. J. H. Verhees, M. M. Wienk, *Adv. Funct. Mater.* **2003**, *13*, 43 – 46.
[34] T. B. Singh, N. Marjanovic, P. Stadler, M. Auinger, G. J. Matt, S. Gunes, N. S. Sariciftci, R. Schwodiauer, S. Bauer, *J. Appl. Phys.* **2005**, *97*, 083714.
[35] B. C. Thompson, Y. G. Kim, T. D. McCarley, J. R. Reynolds, *J. Am. Chem. Soc.* **2006**, *128*, 12714 – 12725.
[36] P. A. van Hal, S. C. J. Meskers, R. A. J. Janssen, *Appl. Phys. A* **2004**, *79*, 41 – 46.
[37] Y.-X. Liu, M. A. Summers, S. R. Scully, M. D. McGehee, *J. Appl. Phys.* **2006**, *99*, 093521.
[38] S. R. Scully, M. D. McGehee, *J. Appl. Phys.* **2006**, *100*, 034907.
[39] H. Ohkita, S. Cook, Y. Astuti, W. Duffy, M. Heeney, S. Tierney, I. McCulloch, D. D. C. Bradley, J. R. Durrant, *Chem. Commun.* **2006**, 3939 – 3941.
[40] T. A. Ford, I. Avilov, D. Beljonne, N. C. Greenham, *Phys. Rev. B* **2005**, *71*, 125212.
[41] J. J. Benson-Smith, L. Goris, K. Vandewal, K. Haenen, J. V. Manca, D. Vanderzande, D. D. C. Bradley, J. Nelson, *Adv. Funct. Mater.* **2007**, *17*, 451 – 457.
[42] V. Chukharev, N. V. Tkachenko, A. Efimov, D. M. Guldi, A. Hirsch, M. Scheloske, H. Lemmetyinen, *J. Phys. Chem. B* **2004**, *108*, 16377 – 16385.
[43] J. W. Arbogast, C. S. Foote, M. Kao, *J. Am. Chem. Soc.* **1992**, *114*, 2277 – 2279.
[44] H. Hoppe, N. S. Sariciftci, *J. Mater. Chem.* **2006**, *16*, 45 – 61.
[45] X. Yang, J. Loos, *Macromolecules* **2007**, *40*, 1353 – 1362.
[46] S. E. Shaheen, C. J. Brabec, N. S. Sariciftci, F. Padinger, T. Fromherz, J. C. Hummelen, *Appl. Phys. Lett.* **2001**, *78*, 841 – 843.
[47] H. Hoppe, M. Niggeman, C. Winder, J. Kraut, R. Hiesgen, A. Hinsch, D. Meissner, N. S. Sariciftci, *Adv. Funct. Mater.* **2004**, *14*, 1005 – 1011.
[48] X. Yang, J. K. J. van Duren, R. A. J. Janssen, M. A. J. Michels, J. Loos, *Macromolecules* **2004**, *37*, 2151 – 2158.
[49] V. Shrotriya, G. Li, Y. Yao, T. Moriarity, K. Emery, Y. Yang, *Adv. Funct. Mater.* **2006**, *16*, 2016 – 2023.
[50] J. M. Kroon, M. M. Wienk, W. J. H. Verhees, J. C. Hummelen, *Thin Solid Films* **2002**, *403–404*, 223 – 228.
[51] M. Reyes-Reyes, K. Kim, J. Dewald, R. Lopez-Sandoval, A. Avadhanula, S. Curran, D. L. Carroll, *Org. Lett.* **2005**, *7*, 5749 – 5752.
[52] K. Kim, J. Liu, M. A. G. Namboothiry, D. L. Carroll, *Appl. Phys. Lett.* **2007**, *90*, 163511.
[53] C.-J. Ko, Y.-K. Lin, F.-C. Chen, C.-W. Chu, *Appl. Phys. Lett.* **2007**, *90*, 063509.
[54] J.-i. Nakamura, K. Murata, K. Takahashi, *Appl. Phys. Lett.* **2005**, *87*, 132105.
[55] C. Yang, J. G. Hu, A. J. Heeger, *J. Am. Chem. Soc.* **2006**, *128*, 12007 – 12013.
[56] F. Padinger, R. S. Rittberger, N. S. Sariciftci, *Adv. Funct. Mater.* **2003**, *13*, 85 – 88.
[57] Y. Kim, S. A. Choulis, J. Nelson, D. D. C. Bradley, S. Cook, J. R. Durrant, *Appl. Phys. Lett.* **2005**, *86*, 063502.
[58] X. Yang, J. Loos, S. C. Veenstra, W. J. H. Verhees, M. M. Wienk, J. M. Kroon, M. A. J. Michels, R. A. J. Janssen, *Nano Lett.* **2005**, *5*, 579 – 583.
[59] X. Yang, A. Alexeev, M. A. J. Michels, J. Loos, *Macromolecules* **2005**, *38*, 4289 – 4295.
[60] G. Li, V. Shrotriya, Y. Yao, Y. Yang, *J. Appl. Phys.* **2005**, *98*, 043704.
[61] P. Peumans, S. Uchida, S. R. Forrest, *Nature* **2003**, *425*, 158 – 162.
[62] V. Shrotriya, Y. Yao, G. Li, Y. Yang, *Appl. Phys. Lett.* **2006**, *89*, 063505.
[63] Y. Zhao, Z. Xie, Y. Qu, Y. Geng, L. Wang, *Appl. Phys. Lett.* **2007**, *90*, 043504.
[64] V. D. Mihailetchi, H. Xie, B. de Boer, L. M. Popescu, L. J. A. Koster, *Appl. Phys. Lett.* **2006**, *89*, 012107.
[65] V. D. Mihailetchi, H. Xie, B. de Boer, L. J. A. Koster, P. W. M. Blom, *Adv. Funct. Mater.* **2006**, *16*, 699 – 708.
[66] T. Erb, U. Zhokhavets, G. Gobsch, S. Raleva, B. Stuhn, P. Schilinsky, C. Waldauf, C. J. Brabec, *Adv. Funct. Mater.* **2005**, *15*, 1193 – 1196.
[67] S. Backer, K. Sivula, D. F. Kavulak, J. M. J. Fréchet, *Chem. Mater.* **2007**, *19*, 2927 – 2929.
[68] K. Sivula, C. K. Luscombe, B. C. Thompson, J. M. J. Fréchet, *J. Am. Chem. Soc.* **2006**, *128*, 13988 – 13989.
[69] P. J. Brown, D. S. Thomas, A. Kohler, J. S. Wilson, J.-S. Kim, C. M. Ramsdale, H. Sirringhaus, R. H. Friend, *Phys. Rev. B* **2003**, *67*, 064203.
[70] Y. Kim, S. Cook, S. M. Tuladhar, S. A. Choulis, J. Nelson, J. R. Durrant, D. D. C. Bradley, M. Giles, I. McCulloch, C.-S. Ha, M. Ree, *Nat. Mater.* **2006**, *5*, 197 – 203.
[71] H. Sirringhaus, P. J. Brown, R. H. Friend, M. M. Nielsen, K. Bechgaard, B. M. W. Langerveld-Voss, A. J. H. Spiering, R. A. J. Janssen, E. W. Meijer, P. Herwig, D. M. de Leeuw, *Nature* **1999**, *401*, 685 – 688.
[72] A. Zen, J. Pflaum, S. Hirschmann, W. Zhuang, F. Jaiser, U. Asawapirom, J. P. Rabe, U. Scherf, D. Neher, *Adv. Funct. Mater.* **2004**, *14*, 757 – 764.
[73] R. J. Kline, M. D. McGehee, E. N. Kadnikova, J. Liu, J. M. J. Fréchet, M. F. Toney, *Macromolecules* **2005**, *38*, 3312 – 3319.
[74] P. Schilinsky, U. Asawapirom, U. Scherf, M. Biele, C. J. Brabec, *Chem. Mater.* **2005**, *17*, 2175 – 2180.
[75] C. Melzer, E. J. Koop, V. D. Mihailetchi, P. W. M. Blom, *Adv. Funct. Mater.* **2004**, *14*, 865 – 870.
[76] M. Kemerink, J. K. J. van Duren, P. Jonkheijm, W. F. Pasveer, P. M. Koenraad, R. A. J. Janssen, H. W. M. Salemink, J. H. Wolter, *Nano Lett.* **2003**, *3*, 1191 – 1196.
[77] V. D. Mihailetchi, L. J. A. Koster, P. W. M. Blom, C. Melzer, B. de Boer, J. K. J. van Duren, R. A. J. Janssen, *Adv. Funct. Mater.* **2005**, *15*, 795 – 801.
[78] J. K. J. van Duren, X. Yang, J. Loos, C. W. T. Bulle-Lieuwma, A. B. Sieval, J. C. Hummelen, R. A. J. Janssen, *Adv. Funct. Mater.* **2004**, *14*, 425 – 434.
[79] K. M. Coakley, M. D. McGehee, *Chem. Mater.* **2004**, *16*, 4533 – 4542.
[80] J. Hou, Z. Tan, Y. Yan, Y. He, C. Yang, Y. Li, *J. Am. Chem. Soc.* **2006**, *128*, 4911 – 4916.
[81] E. Zhou, C. He, Z. Tan, C. Yang, Y. Li, *J. Polym. Sci. Part A* **2006**, *44*, 4916 – 4922.
[82] C. Winder, N. S. Sariciftci, *J. Mater. Chem.* **2004**, *14*, 1077 – 1086.
[83] H. A. M. van Mullekom, J. A. J. M. Vekemans, E. E. Havinga, E. W. Meijer, *Mater. Sci. Eng. R* **2001**, *32*, 1 – 40.
[84] F. Zhang, K. G. Jespersen, C. Björström, M. Svensson, M. R. Andersson, V. Sundström, K. Magnusson, E. Moons, A. Yartsev, O. Inganäs *Adv. Funct. Mater.* **2006**, *16*, 667 – 674.
[85] A. Gadisa, F. Zhang, D. Sharma, M. Svensson, M. R. Andersson, O. Inganas, *Thin Solid Films* **2007**, *515*, 3126 – 3131.
[86] F. Zhang, W. Mammo, L. M. Andersson, S. Admassie, M. R. Andersson, O. Inganäs *Adv. Mater.* **2006**, *18*, 2169 – 2173.
[87] C. Shi, Y. Yao, Y. Yang, Q. Pei, *J. Am. Chem. Soc.* **2006**, *128*, 8980 – 8986.
[88] M. M. Wienk, M. G. R. Turbiez, M. P. Struijk, M. Fonrodona, R. A. J. Janssen, *Appl. Phys. Lett.* **2006**, *88*, 153511.
[89] D. Mühlbacher, M. Scharber, M. Morana, Z. Zhu, D. Waller, R. Gaudiana, C. Brabec, *Adv. Mater.* **2006**, *18*, 2884 – 2889.
[90] M. M. Wienk, J. M. Kroon, W. J. H. Verhees, J. Knol, J. C. Hummelen, P. A. van Hal, R. A. J. Janssen, *Angew. Chem.* **2003**, *115*, 3493 – 3497; *Angew. Chem. Int. Ed.* **2003**, *42*, 3371 – 3375.

[91] F. B. Kooistra, V. D. Mihailetchi, L. M. Popescu, D. Kronholm, P. W. M. Blom, J. C. Hummelen, *Chem. Mater.* **2006**, *18*, 3068 – 3073.
[92] Y. Yao, C. Shi, G. Li, V. Shrotriya, Q. Pei, Y. Yang, *Appl. Phys. Lett.* **2006**, *89*, 153507.
[93] L. M. Andersson, O. Inganas, *Appl. Phys. Lett.* **2006**, *88*, 082103.
[94] X. Wang, E. Perzon, F. Oswald, F. Langa, S. Admassie, M. R. Andersson, O. Inganas, *Adv. Funct. Mater.* **2005**, *15*, 1665 – 1670.
[95] L. Zheng, Q. Zhou, X. Deng, M. Yuan, G. Yu, Y. Cao, *J. Phys. Chem. B* **2004**, *108*, 11921 – 11926.
[96] L. M. Popescu, P. van't Hof, A. B. Sieval, H. T. Jonkman, J. C. Hummelen, *Appl. Phys. Lett.* **2006**, *89*, 213507.
[97] I. Riedel, E. von Hauff, J. Parisi, N. Martin, F. Giacalone, V. Dyakonov, *Adv. Funct. Mater.* **2005**, *15*, 1979 – 1987.
[98] Y. Shao, Y. Yang, *Adv. Mater.* **2005**, *17*, 2841 – 2844.
[99] F. Guo, Y.-G. Kim, J. R. Reynolds, K. S. Schanze, *Chem. Commun.* **2006**, 1887 – 1889.
[100] V. D. Mihailetchi, L. J. A. Koster, J. C. Hummelen, P. W. M. Blom, *Phys. Rev. Lett.* **2004**, *93*, 216601.
[101] L. J. A. Koster, V. D. Mihailetchi, P. W. M. Blom, *Appl. Phys. Lett.* **2006**, *88*, 052104.
[102] M. M. Mandoc, L. J. A. Koster, P. W. M. Blom, *Appl. Phys. Lett.* **2007**, *90*, 133504.
[103] V. D. Mihailetchi, J. Wildeman, P. W. M. Blom, *Phys. Rev. Lett.* **2005**, *94*, 126602.
[104] K. Sivula, Z. T. Ball, N. Watanabe, J. M. J. Fréchet, *Adv. Mater.* **2006**, *18*, 206 – 210.
[105] M. Drees, H. Hoppe, C. Winder, H. Neugebauer, N. S. Sariciftci, W. Schwinger, F. Schaffler, C. Topf, M. C. Scharber, Z. Zhu, R. Gaudiana, *J. Mater. Chem.* **2005**, *15*, 5158 – 5163.
[106] J.-F. Nierengarten, S. Setayesh, *New J. Chem.* **2006**, *30*, 313 – 316.
[107] Z. Zhu, S. Hadjikyriacou, D. Waller, R. Guadiana, *J. Macromol. Sci. Pure Appl. Chem.* **2004**, *41*, 1467 – 1487.
[108] K. A. Murray, A. B. Holmes, S. C. Moratti, G. Rumbles, *J. Mater. Chem.* **1999**, *9*, 2109 – 2115.
[109] P. Schilinsky, C. Waldauf, C. J. Brabec, *Adv. Funct. Mater.* **2006**, *16*, 1669 – 1672.
[110] U. Stalmach, B. de Boer, C. Videlot, P. F. van Hutten, G. Hadziioannou, *J. Am. Chem. Soc.* **2000**, *122*, 5464 – 5472.
[111] J. Y. Kim, S. H. Kim, H.-H. Lee, K. Lee, W. Ma, X. Gong, A. J. Heeger, *Adv. Mater.* **2006**, *18*, 572 – 576.

